The European Forest Disturbance Atlas: a forest disturbance monitoring system using the Landsat archive

Alba Viana-Soto[1], Cornelius Senf[1]

[1]Technical University of Munich, School of Life Sciences, Earth Observation for Ecosystem Management, Hans-Carl-von-Carlowitz-Platz 2, 85354 Freising, Germany

Correspondence to: Alba Viana-Soto (alba.viana-soto@tum.de)

Abstract

Forests in Europe are undergoing complex changes that require a comprehensive monitoring of disturbance occurrence. Here we present the European Forest Disturbance Atlas (EFDA), a Landsat-based approach for mapping annual forest disturbances across continental Europe since 1985. We built a consistent Landsat data cube of summer composites and compiled reference data on forest land use and forest disturbances. A classification-based approach was developed to detect forest disturbances annually, therefore accounting for multiple disturbance events per time-series. The EFDA contains annual layers on disturbance occurrence, severity and agent, as well as aggregated layers on the number of disturbances and the latest and greatest disturbance year. Based on the annual disturbance estimates (1985-2023), we quantified a total forest disturbed area of 439,000 km^2, increasing to 610,000 km^2 when accounting for multiple overlapping disturbance events. Map accuracies of the disturbance classification showed an overall F1-score of 0.89, with very low errors (<1%) for the undisturbed class and with commission and omission errors for the disturbed class of 17.3% and 22.5%, respectively. Further, temporal validation revealed errors decreased over time, with commission substantially decreases to 10.6% after the year 2000. The workflow implemented to create annual forest disturbance maps was designed for easy updating when new data arrives and in an open access framework to facilitate reproducibility, thus paving the road for an operational forest disturbance system in Europe. EFDA products are available at https://doi.org/10.5281/zenodo.13333034 (Viana-Soto and Senf, 2024).

1. Introduction

Europe's forests cover more than one third of the continent and they provide essential ecosystem services to society (FOREST EUROPE, 2020), spanning from timber production and carbon storage (Lindner et al., 2010) ~~over~~ water purification and regulation (Orsi et al., 2020), to recreation and spiritual value (Saarikoski et al., 2015). Europe's forests are shaped by a long history of forest management, with past management decisions driving their current structure and composition (Ciais et al., 2008; Sabatini et al., 2018; Seidl and Senf, 2024). Past forest management has also focussed on increasing forest resistance to natural disturbances (Seidl, 2014), sustaining a continuous provision of timber and other ecosystem services (Thom and Seidl, 2016). In the recent years, however, evidence for changing natural disturbance regimes has been reported globally (McDowell

et al., 2020) and also in Europe, climate change and climate extremes have led to increased natural disturbances (Patacca et al., 2023; Senf et al., 2018; Senf and Seidl, 2021b). The trend of increasing natural disturbances coincides with an increasing demand for wood globally, with reported increases in timber harvest rates observed across most of Europe (Breidenbach et al., 2022; Ceccherini et al., 2020; Palahí et al., 2021; Seidl and Senf, 2024). Forests in Europe are thus undergoing complex changes that require a fundamental monitoring of where and when disturbances occur, providing a basis for decision making and forest planning.

Remote sensing data can provide detailed and consistent information on forests (Hirschmugl et al., 2017; Senf, 2022), and the Landsat archive (Wulder et al., 2022) – covering more than four decades – plays a key role in characterizing disturbances (Banskota et al., 2014). In particular, Landsat contributed to a better understanding of the causes and consequences of changing disturbance regimes in Europe (Grünig et al., 2022; Lecina-Diaz et al., 2024; Senf and Seidl, 2018; Sommerfeld et al., 2018; Stritih et al., 2021) and on disturbance interactions (Buma, 2015; Hermosilla et al., 2019; Turner and Seidl, 2023). Since the opening of the Landsat archive, different methodologies and algorithms have emerged for monitoring forest cover change across large areas (Zhu, 2017), with a regional focus on forests of the United States and Canada (Kennedy et al., 2010; Verbesselt et al., 2010; Zhao et al., 2019; Zhu and Woodcock, 2014b). Such forest change detection algorithms can broadly be grouped into four types: (1) trajectory segmentation approaches (Hughes et al., 2017; Kennedy et al., 2010; Moisen et al., 2016), (2) time series decomposition approaches (Verbesselt et al., 2010; Zhao et al., 2019), (3) threshold-based methods (Huang et al., 2010), and (4) classification approaches (Hansen et al., 2013; Hermosilla et al., 2015). Time series segmentation or decomposition methods rely on the detection of statistical breakpoints in a spectral time series to detect forest change. While easy to implement and requiring little to no reference data, such approaches make use of only a limited set of spectral characteristics (usually one spectral index) and they require re-calibration when new observations are incorporated (Hermosilla et al., 2017). Threshold-based methods, in turn, can be easily updated with new data but they rely on simple thresholds that might be difficult to apply across different ecosystems, because thresholds will vary depending on forest composition and site conditions (Cardille et al., 2022). Classification-based methods, particularly machine learning-based approaches (Belgiu and Drăguţ, 2016), can capture complex patterns and adapt to different types of disturbances and varying environmental conditions (Cardille et al., 2022). This makes them more flexible to map changes across large areas (Hansen et al., 2013). Classification-based approaches also apply a strict definition of disturbances (i.e. by a well-defined classification label) and they can reliably reduce commission errors resulting from noise in the time series (Cohen et al., 2017; Hermosilla et al., 2015). Finally, annual classification approaches can also facilitate the detection of more than one disturbance per pixel time series, which can be challenging with trajectory-based approaches (Hermosilla et al., 2015).

Due to the rapid development of new remote sensing approaches, there is growing interest to also develop operational forest monitoring systems at the level of the European Union (Fassnacht et al., 2024; Ferretti, 2024; Ferretti et al., 2024; Nabuurs et al., 2022) and in particular for the monitoring of tree cover change and disturbance (Dutrieux et al., 2023; European Commission et al., 2023). As global tree cover change products contain high uncertainty when analyzed regionally (Ceccherini

et al., 2020, Breidenbach et al., 2022; Palahí et al., 2021), efforts have been made to develop forest disturbance monitoring approaches specifically for Europe (Francini et al., 2021; Senf and Seidl, 2021a; Turubanova et al., 2023). Francini et al. (2021) proposed an automated algorithm (3I3D) for mapping forest disturbances based on spectral change in three indices within three consecutive years. The approach has shown good results for harvest disturbance detection in Italy but was yet not applied at continental scale. Shortly after, Senf and Seidl (2021a) created the first pan-European characterization of forest disturbance by combining a trajectory-segmentation algorithm (LandTrendr; Kennedy et al., 2010) with a random forest classification approach to filter out false positives from the LandTrendr segmentation (Cohen et al., 2018). While delivering spatially consistent data across Europe, this approach was constrained to the greatest change event per pixel and thus cannot include multiple disturbances per pixel. Turubanova et al. (2023) modelled changes in tree crown height across Europe from 2001 to 2021 by integrating Landsat imagery and Lidar data (ALS and GEDI). It constitutes the first attempt to analyse the evolution of tree canopy height at the European scale, but it only includes data from 2001 onwards and thus lacks a baseline for understanding more recently observed changes and for quantifying trends over time. As such, while there is a multitude of different approaches and products mapping forest disturbance across Europe, none of the existing approaches fulfils all requirements for an operational monitoring of forest change in Europe.

We here present the European Forest Disturbance Atlas (EFDA), which is a Landsat-based approach for mapping annual forest disturbances across continental Europe since 1985. The EFDA contains annual layers on disturbance occurrence, severity and agent, as well as aggregated layers on the latest and greatest disturbance year and on the number of disturbances. The aim of this paper is to (i) explain and document the data and processing routines used for Landsat-based disturbance mapping, (ii) quantify uncertainties and errors in the disturbance maps, (iii) describe the individual map products derived from the disturbance maps, and (iv) discuss the use (and misuse) of the EFDA for forest monitoring.

2. Data and Methods

The overall workflow behind the EFDA contains six processing steps summarized in Figure 1 and described in full detail in the following sub-sections: First, building a consistent Landsat data cube for Europe. Second, compiling a reference dataset on forest land use and forest disturbances. Third, creating a consistent forest land use mask. Fourth, developing a classification-based approach to detect disturbances annually at the pixel level. Following this, validating the forest land use mask and disturbances maps based on an independent reference sample. Fifth, identifying disturbance patches and the likeliest agent of disturbance at the patch level. Lastly, creating a set of summary layers on forest disturbances and forest disturbance agents.

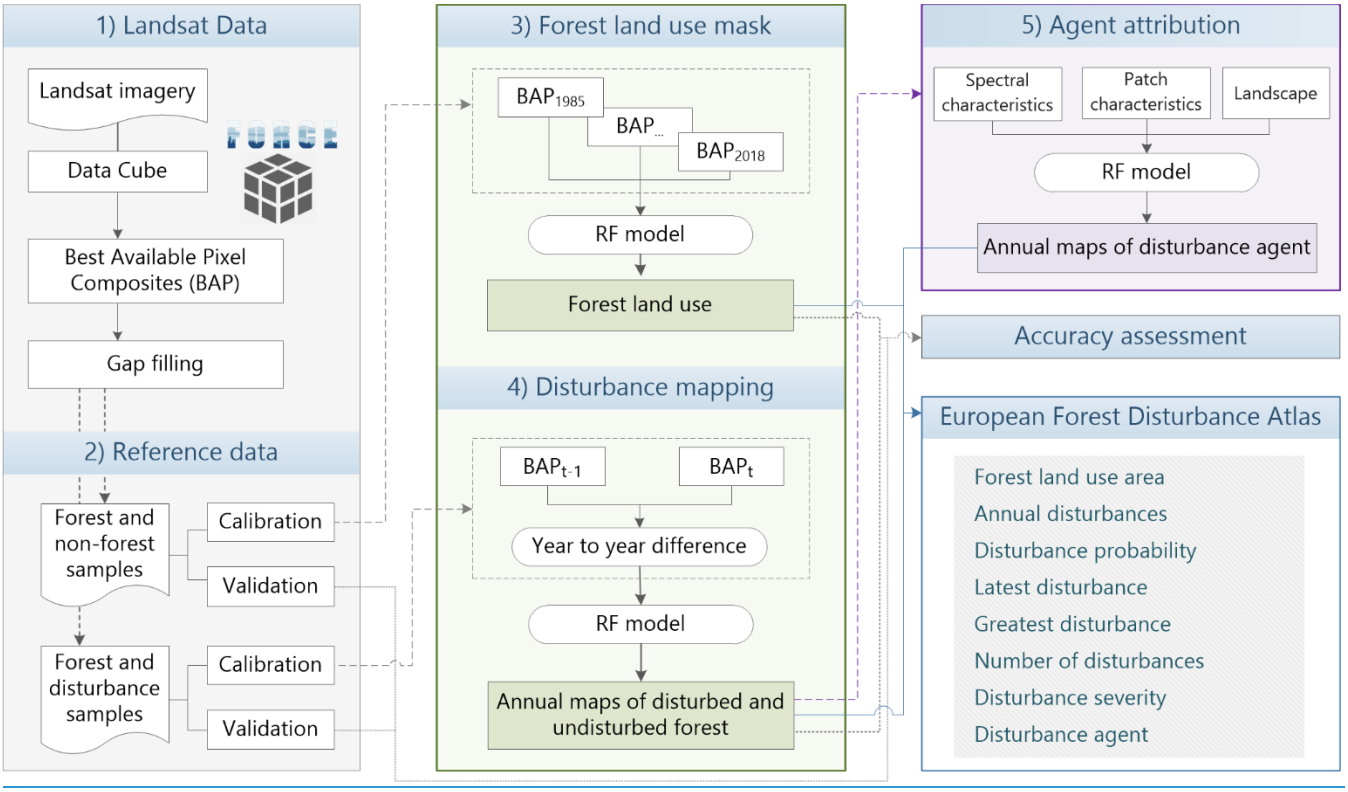

Figure 1. Overview of the workflow for creating the European Forest Disturbance Atlas.

2.1. Landsat data cube

Our analysis area covers continental Europe, which was defined as all European countries except for Russia, Malta, Cyprus and overseas territories and which covers a total of 5,749,424 km^2 of land area. For the analysis area, we identified all Level-1 images collected from Landsat 4 to Landsat 9 since 1984 and with a cloud cover below 60 %. We only searched for images within the growing season (1st June and 30th September) to prevent differences in reflectance caused by phenological variations and sun angle changes. This resulted in a total of 115,663 images until 2023, which we downloaded from the United States Geological Survey (Figure 2a). The Level-1 Landsat images were further processed to surface reflectance (Level-2) and organized in a data cube structure of non-overlapping tiles of 150 x 150 km (Figure 2b) using the Framework for Operational Radiometric Correction for Environmental Monitoring (FORCE version 3.7.9, Frantz, 2019). Processing steps included atmospheric corrections using a precompiled water vapor database (Frantz et al., 2016), topographic correction using the ASTER Global Digital Elevation Model Version 3 (Abrams et al., 2020), bidirectional reflectance distribution function corrections, as well as cloud and cloud shadow masking (Frantz et al., 2016; Roy et al., 2016; Zhu and Woodcock, 2012). Topographic normalization is performed by applying a modified C-correction (Kobayashi and Sanga-Ngoie, 2008), which is a physically based correction of topography, amended by an empirically derived extra parameter C (Hantson and Chuvieco,

2011). Cloud masking is applied using a modified version of Fmask with additional steps that enhance cloud and shadow detection (Frantz et al., 2016). After detecting clouds and cloud shadows in every Landsat image independently by using the Fmask algorithm, a time-series algorithm is applied to detect outliers and remove additional clouds and shadows on a per-pixel basis (Frantz et al., 2015; Zhu and Woodcock, 2014a).

From the Level-2 data cube, we created annual, cloud-free best available pixel composites across the whole analysis area. Best available pixel compositing has been demonstrated to yield temporally and radiometrically consistent data for large area mapping (Hermosilla et al., 2022), and recent research has shown their superiority in detecting disturbances compared to other temporal aggregation methods (Francini et al., 2023). For creating the best available pixel composites, we selected for each pixel the best observations based on a parametric weighting scheme established in previous research (Griffiths et al. 2013). Observations were ranked per pixel according to distance to clouds and cloud shadows, haze opacity and proximity to a predefined target date (1st of August; Figure A1- Appendix). Each of these factors is assigned a specific weight in the scoring algorithm and only high-quality pixels are considered, i.e. observations with very low cloud or haze score are discarded. The observation with the highest cumulative score is then selected as the best pixel for each location, ensuring both spectral and temporal consistency in the composites. As there were still remaining gaps in the composites (i.e., areas where no high-quality observation was found during the summer season, 10.1% of the total area on average (see Figure A2 - Appendix for annual details), we applied a linear gap-filling algorithm extrapolating the previous year's spectral values to fill remaining gaps (Figure 2c), reducing data gaps to 4.9% per year on average.

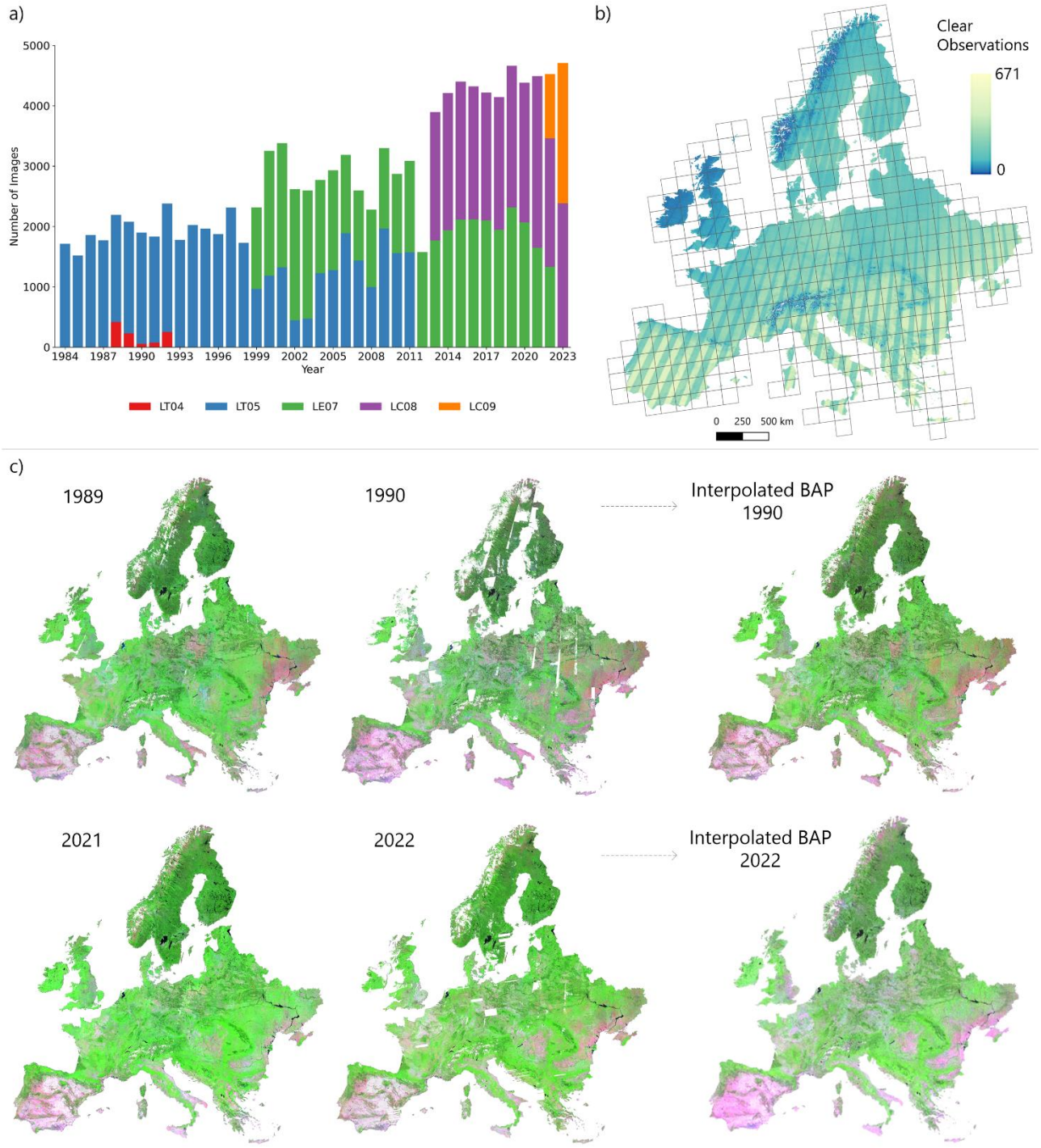

Figure 2. a) Number of images processed per year and sensor (1984-2023). b) Clear Sky Observations across Europe for the entire time series and tile system of the data cube. c) Examples of best available pixel (BAP) composites (RGB: SWIR2/NIR/Red) for Europe and resulting composites after gap-filling.

2.2. Reference data for disturbance mapping

We compiled reference data for both forest and non-forest land use pixels, used to train a classifier that discriminates forest from other land use, as well as for disturbance and undisturbed pixels, used to train a classifier that detects tree cover change within forest land use annually. For the latter, we used a previously established dataset of 20,084 manually interpreted Landsat pixels for 35 countries available in https://zenodo.org/records/3561925. The dataset was built from two samples: The first one containing 24,000 randomly selected Landsat pixels for six countries across all land uses for the period 1985 to 2017 (Central Europe; Senf et al., 2018). The second one containing 500 randomly selected Landsat pixels for 29 countries (excluding Central Europe) within forest land use for the period 1985 to 2018 (Senf et al., 2021). After removing non-forest land use pixels from both samples, we were left with a total of 20,084 reference pixels within forest land use across Europe (Figure A3 - Appendix). For each pixel, trained interpreters segmented the spectral time series into linear segments of stable, disturbance and recovery (Figure 3) using an established interpretation tool (Cohen et al., 2010). Using Landsat images and high-resolution imagery available in Google Earth, the interpreters can determine whether spectral changes correspond to forest canopy changes or whether spectral changes were caused by other artifacts, such as clouds, illumination conditions or phenological variations. The interpreters additionally recorded the land cover for each node of each segment (tree [>=50% tree cover] or non-treed [<50% tree cover]), which allowed us to disentangle stand-replacing disturbances (land cover changes from treed to non-treed) from non-stand-replacing disturbances (land cover stays treed despite disturbance). For full details on the interpretation, we direct the reader to the original publications (Senf et al., 2018, 2021). We converted the linear segments into annual binary information on disturbance occurrence (Figure 3), which yielded 662,772 data points (pixel-year combinations) to train an annual classification model.

For masking out all non-forest land use, we complemented the above sample within forest land use with non-forest land uses reference points from the LUCAS database (Land Use and Coverage Area frame Survey, Eurostat: https://ec.europa.eu/eurostat/web/lucas). The LUCAS database is a spatially explicit database using a stratified random sampling design and trained field surveyors to assess land use and land cover (among other parameters) at 651,676 locations across Europe over the years 2006 to 2018 (d'Andrimont et al., 2020). LUCAS has been successfully used for land cover mapping (Pflugmacher et al., 2019) and thus is an ideal database for generating reference information for large-scale remote sensing analyses. From LUCAS, we extracted samples on the following categories: artificial land, croplands, grassland, bare land, water, and wetlands. We used only direct observations made at the plot in the field or via photointerpretation for which the land cover area was >1 ha, the land cover proportion was >80%, and plots for which the field-observed GPS location was <15m away from the LUCAS point. We collected a total of 46,651 non-forest reference pixels that way, matching the forest to non-forest land use ratio per country following statistics available in the FAOSTATS database (FOREST EUROPE, 2020). Doing so yields a random sample per country, i.e. the share of samples within and outside forest land use corresponds to the share of forest to non-forest land use of the country.

From both samples, a validation subsample of 2500 pixels each was retained for independent validation of the forest land use and forest disturbance classification. The land use validation sample was drawn proportionally to each countries land area and stratified by forest share within each country (see Table 1), which emulates a random sample across Europe's land area. That said, due to the absence of LUCAS information for 10 countries, the non-forest sample was slightly smaller (2066 samples) than the planned 2500 samples (see Table 1). The forest disturbance validation sample was drawn proportionally to each countries forest area, which emulates a random sample across Europe's forest area. Both samples are thus independent, random draws from the full population and allow for estimating unbiased map accuracies of the final map products.

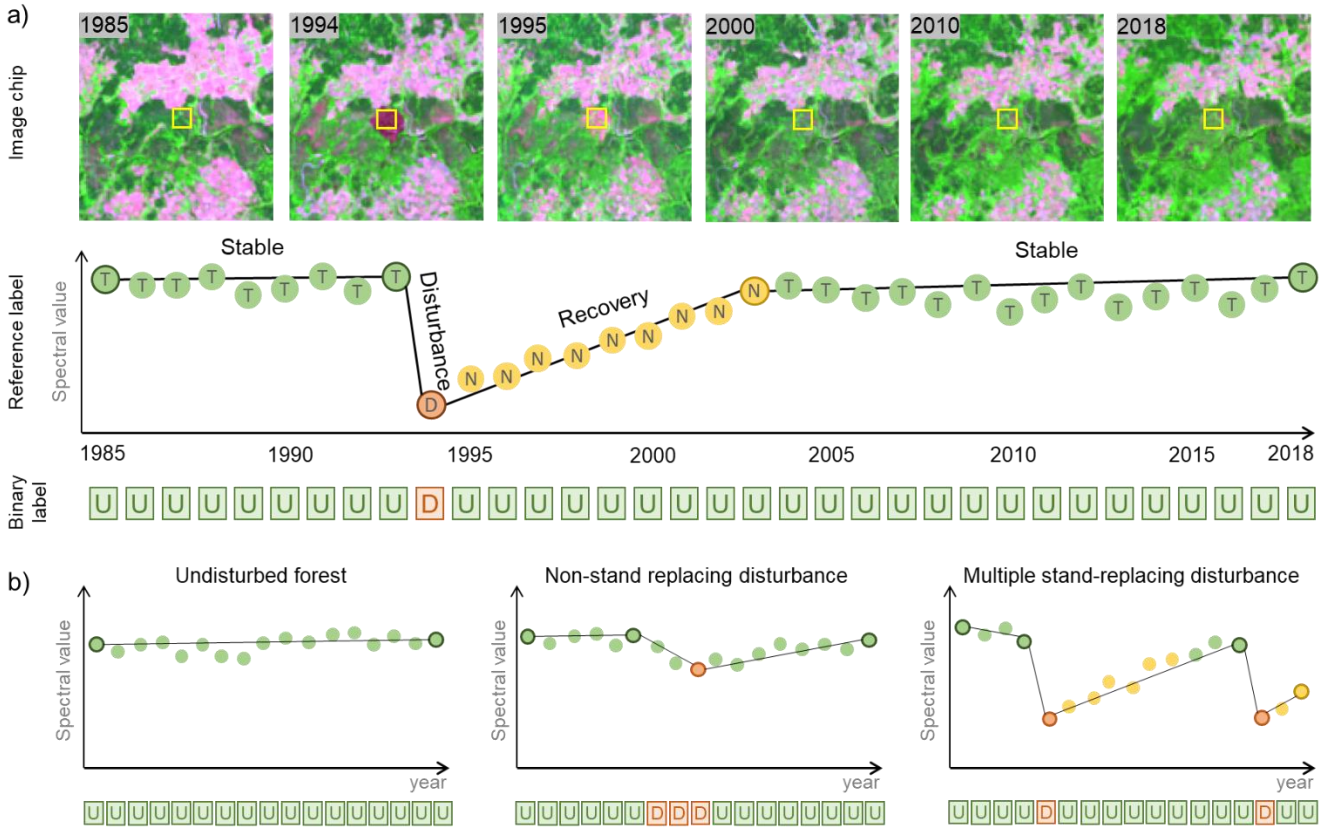

Figure 3. Schematic representation of the original reference data from Senf et al. 2018 and Senf et al. 2021: a) Image chips and corresponding segmentation labels of stable forest, disturbance and recovery segments and corresponding land cover of treed (T) and non-treed (N), ultimately labelled into annual binary classes of Undisturbed (U) and Disturbed (D); b) examples of undisturbed forest, a gradual non-stand replacing disturbance and multiple stand-replacing disturbances, and their corresponding binary labels.

Table 1. Sizes of the validation samples for the land use and disturbance classifications and the corresponding weights used for calculating the sample size (missing samples in the LUCAS database indicated by "-")

Country name	Country area (km2)	Forest area (km2)	Land area proportion	Forest area proportion	Land use validation sample		Disturbance validation sample
					forest	non-forest	forest
Albania (AL)	28786.07	7716	0.00501	0.268	3	-	9
Austria (AT)	83988.21	39600	0.01461	0.471	17	20	47
Belarus (BY)	207575.27	80334	0.03610	0.387	35	-	96
Belgium (BE)	30587.77	6834	0.00532	0.223	3	10	8
Bosnia and Herzegovina (BA)	51030.41	25599	0.00888	0.502	11	-	31
Bulgaria (BG)	110953.91	36250	0.01930	0.327	16	32	43
Croatia (HR)	57017.2	24901	0.00992	0.437	11	14	30
Czechia (CZ)	78842.74	26000	0.01371	0.330	11	23	31
Denmark (DK)	43501.59	6120	0.00757	0.141	3	16	7
Estonia (EE)	45405.32	23066	0.00790	0.508	10	10	27
Finland (FI)	338434	233320	0.05886	0.689	101	46	278
France (FR)	549006.24	246640	0.09549	0.449	107	132	294
Germany (DE)	357454.99	114190	0.06217	0.319	50	105	136
Greece (EL)	124885.96	37600	0.02172	0.301	16	38	45
Hungary (HU)	93001.36	20990	0.01618	0.226	9	31	25
Ireland (IE)	70243.37	7540	0.01222	0.107	3	28	9
Italy (IT)	300887.48	106736	0.05233	0.355	46	85	127
Latvia (LV)	64549.9	28807	0.01123	0.446	12	16	34
Lithuania (LT)	64941.46	21223	0.01130	0.327	9	19	25
Moldova (MD)	33847.27	3290	0.00589	0.097	1	-	4
Montenegro (ME)	13764.39	6252	0.00239	0.454	3	-	7
Netherlands (NL)	35162.75	3650	0.00612	0.104	2	13	4
North Macedonia (MK)	25438.31	10285	0.00442	0.404	4	-	12
Norway (NO)	311654.47	121120	0.05421	0.389	53	-	145
Poland (PL)	311759.97	90000	0.05422	0.289	39	97	107
Portugal (PT)	88700.69	31820	0.01543	0.359	14	25	38
Romania (RO)	238289.83	69610	0.04145	0.292	30	74	83
Serbia (RS)	88372.28	27200	0.01537	0.308	12	-	32
Slovakia (SK)	49036.66	20006	0.00853	0.408	9	12	24
Slovenia (SI)	20221.19	12574	0.00352	0.622	6	3	15
Spain (ES)	498518.52	184180	0.08671	0.369	80	136	219
Sweden (SE)	450040.79	280730	0.07828	0.624	122	74	335
Switzerland (CH)	41239.21	12540	0.00717	0.304	5	-	15
Ukraine (UA)	597120.26	105000	0.10386	0.176	46	-	124
United Kingdom (UK)	245164.44	28650	0.04264	0.117	13	94	34
					912	1154	2500
					2066		

2.3. Forest land use mask

A forest land use mask was required to mask out any non-forest land use areas, which often exhibit strong spectral changes that could be confused with disturbances. Since there is no consistent forest land use mask available across all continental Europe, we created our own forest land use mask using a multitemporal classification approach. We broadly followed the FAO definition of forest land use, which is any area that has or will reach tree cover greater 10% in the near future, is larger than 0.5 ha and 20 m in width, and which is primarily not used under urban or agricultural land use (FAO, 2020). This definition thus includes young forests of lower tree cover, areas of reforestation and temporally unstocked areas (e.g. forestry roads). To match this definition, we assigned each reference pixel (see Section 2.2.) that has been treed (even temporally) since 1985 as forest land use. All reference pixels of other land uses (i.e. artificial, croplands, water bodies) were assigned to non-forest land use. We use such a broad land use definition, instead of a recent tree cover map, to avoid masking recently disturbed areas that are temporally unstocked but still considered forest land use. Using the reference categories assigned to each pixel, we trained a random forest model with a stack of all annual best available pixel composites as input, ~~(i.e.~~ comprising 34 years with 6 spectral layers and 6 spectral indices (Table 1), resulting in 408 features ~~(~~, see Figure A4 for a visualization of the feature space and Figure A6 for further details on variable importance). We then applied the model to the raster stack to yield one classification of forest/non-forest land use for our entire study period. According to the FAO definition, we also defined a minimum mapping unit (MMU) consisting of 6 Landsat pixels for the forest mask (0.54 ha), converting smaller patches to non-forest. All non-forest land use pixels were excluded from following analyses.

2.4. Annual disturbance mapping

For each forest land use pixel, forest disturbances were classified on an annual basis since 1985. Disturbed and undisturbed forests have a distinctive spectral signal across a two-year period, as spectral characteristics change significantly during disturbance while they remain constant for undisturbed forests (Kennedy et al., 2007). We hence calibrated a random forest model to identify disturbed and undisturbed pixels using the spectral information from a given year (target year t_0) and the previous year (reference year, t_{-1}) to disentangle inter-annual stability and change. As classification input we used a set of spectral indices (NDVI, Tucker, 1979 and NBR, García and Caselles, 1991), the Tasseled Cap components (Baig et al., 2014; Crist, 1985), and the Disturbance Index (Healey et al., 2005) (Table A1, Figure A5 and see Figure A6 for further details on variable importance). As reference we used undisturbed and stand-replacing disturbances (i.e. disturbances that led to a change in land cover; see Section 2.2), which indicate a clear opening of the top canopy and thus allow the model to learn the distinct spectral differences between undisturbed and disturbed pixels. The trained model was then applied annually, which facilitates updating the map product as soon as images are available for the next year.

Due to the imbalanced nature of the sample (disturbances representing only 3%), we applied the SMOTE method (Chawla et al., 2002), which helps by lowering the overall learning cost, assigning higher costs to misclassifying the minority class, and balancing the data through under-sampling the majority and over-sampling the minority class. We further used the module

RandomizedSearchCV (Pedregosa et al., 2011) to efficiently find the best set of hyperparameters using cross-validation, selecting the combination that resulted in the highest area under the receiver operating characteristic curve score. To classify the probability of disturbance into the binary categories disturbed and undisturbed, we optimized the probability cutoff using the F1-score derived from cross-validation. The optimal threshold was 0.5 with an overall F1-score of 91%.

Finally, we applied several post-processing steps: First, annual maps were masked according to the forest land use ~~classification~~ mask (MMU=0.54 ha) and a minimum mapping unit of 3 Landsat pixels was assigned (0.27 ha), reducing the number of single false positive pixels (so-called *salt-and-pepper* effect typical for pixel-based classification). Second, we applied a collapsing step in which multiple disturbances detected in a time window of <4 years since the last disturbance were reduced to the first year the disturbance sequence was detected (Figure 4). This was done to avoid illogical changes (i.e. disturbance, no disturbance, disturbance) and double counting of disturbances in consecutive years that arise from the same disturbance event. That is, if a disturbance event extends over multiple, consecutive years, we will map only the first year of the disturbance segment as disturbed.

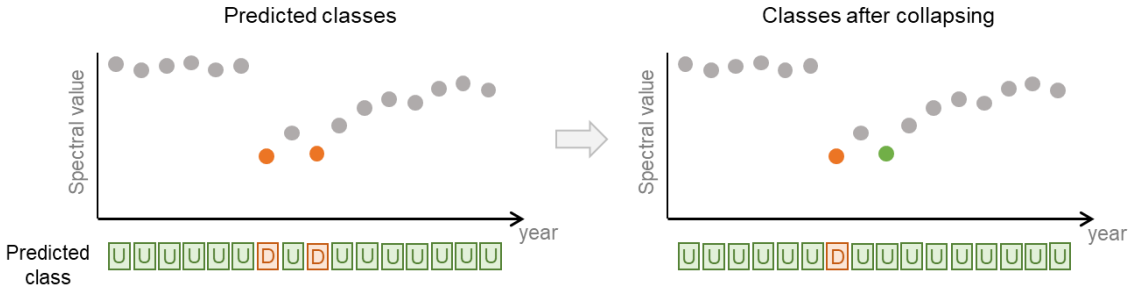

Figure 4. Schematic view of collapsing step to relabel illogical and consecutive disturbance events.

2.5. Accuracy ~~and uncertainty~~ assessment

Robust estimation of map accuracies is important for map uptake and subsequent analyses (Olofsson et al., 2014). We quantified map accuracies of both the forest land use and forest disturbance maps using the independent samples described in 2.2 and standard confusion matrices, from which we estimated omission errors/producer's accuracies (or recall), commission errors/user's accuracies (or precision) and overall errors/accuracies and F1-scores (Forman and Scholz, 2010). Uncertainties in each accuracy estimate were quantified using bootstrapping with 1000 repetitions, which simulates sampling variability due to hypothetical repeated sampling for each estimate. We further assessed how accuracies of the disturbance map varied spatially and temporally. For assessing spatial variability, we computed confusion matrices per region (North - 7 countries, Central - 20 countries, and South - 11 countries), according to FOREST EUROPE 2020 definitions). For assessing temporal variability, we computed confusion matrices and corresponding accuracy estimates per year and for different periods. We also calculated confusion matrices using only stand-replacing disturbances (i.e. pixels where the interpreter assigned a change in land cover) and both stand-replacing and non-stand-replacing disturbances (i.e. pixels where the interpreter assigned no change

in land cover). We did so to test the sensitivity of our maps and map accuracies to low-severity disturbances. Further, we compared the forest land use area estimated from our map to national level statistics on forest land use area obtained from the FAOSTATS database (FOREST EUROPE, 2020). We finally compared our disturbance estimates to existing datasets for Europe (Hansen et al., 2013; Senf and Seidl, 2021a; Turubanova et al., 2023).

2.6. Agent attribution

To identify the most likely agent of disturbances, we adapted an existing attribution algorithm (Sebald et al., 2021; Seidl and Senf, 2024; Senf and Seidl, 2021b) for the annual disturbance maps. The algorithm first detects disturbance patches by grouping pixels disturbed in the same year that are connected by an edge or corner using queen-contiguity. That is, the analysis is performed at the patch-level and not at the pixel level anymore, allowing us to derive patch-level predictors important for disturbance agent attribution (Oeser et al., 2017; Sebald et al., 2021; Stahl et al., 2023). To correct for timing errors in the disturbance map (e.g., a fire mappedspreading over two years might appear as two separate fires), patches from consecutive years that share an edge are merged, with the disturbance year assigned based on a majority vote (see Senf and Seidl 2021b for details). For each patch, we generated a set of 18 predictors, including its size, shape, spectral characteristics, and surrounding landscape (see Table 2 for details and Figure A6 for further details on variable importance, as well as (Seidl and Senf, 2024; Senf and Seidl, 2021b).

Table 2. Predictors used in the agent attribution model

Predictor group	Predictor	Description
Spectral characteristics	Spectral change (NBR, TCB, TCG and TCW)	The mean, standard deviation and maximum value in the respective spectral index during the disturbance event.
Patch characteristics	Patch size and perimeter	The total size of the disturbance patch in ha and perimeter (total number of boundary pixels for the patch)
	Patch fractional dimension index	The fractional dimension index, given an indication of patch complexity, with larger values indicating more complex patches.
Landscape	Pulse-dynamics	The proportion of disturbances in a 5 km radial buffer occurring in the same year as the focal patch. The values range between zero and one, with zero indicating no other disturbances in the same year in the 5 km neighbourhood (high spatiotemporal segregation), whereas a value of one indicates that all other disturbances in the surrounding neighbourhood occurred in the same year (high spatiotemporal clustering).
	Number of patches	Overall number of patches in the 5 km radial buffer.

As reference data, we used an extended reference database of 12,571 points for fires, windthrows, and bark beetle disturbances. This database builds upon an existing reference database of 11,364 points of fires and windthrows developed in (Senf & Seidl , (2021b), and which was extended to 12,571 points to also including bark beetle disturbances (Seidl & Senf, 2024). This dataset was created by combining visual interpretation of an existing disturbances map (Senf and Seidl, 2021a), Landsat data

and high-resolution imagery with different databases on storms (FORWIND, Forzieri et al., 2020), insect outbreaks (DEFID2, Forzieri et al., 2023) and fire related disturbances (EFFIS, https://forest-fire.emergency.copernicus.eu/). Additionally, papers documenting bark beetle outbreaks in Europe were used to support the interpretation of bark beetle patches (Hlásny et al., 2021). Each point in the reference database was linked to a disturbance patch in our disturbance map by a unique patch id. In some cases, two or more occurrence points fell within the same disturbance patch (especially for large fires or windthrows), which reduced the number of patches with an agent label to 12,314 (10,114 for windthrow, 1,085 for bark beetles and 1,115 for fire). The database thus covers the three most important natural disturbance agents in Europe (Patacca et al., 2023). We note, however, that the focus of the attribution is on the root cause of disturbance. That is, an area affected by natural disturbances (e.g. wind) that is salvage logged afterwards is considered a wind disturbance. We did not have dedicated information on harvest in the reference database, because there is no reliable spatially explicit information on harvest activities and interpreting harvest is difficult, because harvest can happen in reaction to natural disturbances (i.e. salvage logging). We thus used an approach developed in Senf and Seidl (2021b) and selected a random background sample from all disturbance patches to indicate the absence of fire, windthrow or bark beetle outbreaks in the model. As harvest is assumed to be the major disturbance agent in Europe (Patacca et al., 2023; Seidl and Senf, 2024), this background sample will represent harvest conditions in contrast to the agent information available in the existing databases. In essence, this approach is similar to presence-only species distribution models, where absence data is also rare (Valavi et al., 2022). We drew a total of 12,314 random patches to represent harvest, equalling to the sum of wind, fire and bark beetle disturbances, and resulting in a final reference database of 24,628 patches. We following trained a random forest model using the agent labels in the reference database and predictors described above. We initially trained a model classifying each patch into one of the four agent categories (wind, fire, bark beetle and harvest) but found high confusion between wind and bark beetle disturbances. This was mostly due to bark beetle reference data being available mostly for very recent, large-scale bark beetle outbreaks in Central Europe that resemble past windthrows in their form and shape. Since less historic information was available on bark beetle disturbances that could have improved model skill, we decided to group wind and bark beetle disturbances into one category. Ecologically, both disturbance agents form a disturbance complex with wind disturbances often triggering bark beetle disturbances and vice versa (Seidl and Rammer, 2017). That said, as bark beetle has been a less important natural disturbance agent compared to wind and fire disturbances prior to the recent Central European drought event (Patacca et al., 2023), disturbances in the wind/bark beetle category prior to 2017 can be considered as mostly wind dominated, while disturbances in the same class can be considered bark beetle dominated after 2017. Finally, as there was no independent sample of reference data available at the agent level, we were unable to provide map accuracies on the resulting agent maps. We through provide model accuracies derived from a fivefold spatial block cross-validation (Valavi et al., 2019) with class errors for each class. Those model accuracies should be taken with caution, because they do not represent true map accuracies.

2.7. Summary layers

Using the annual maps of disturbances and the underlying spectral information, we computed a series of layers that compose the European Forest Disturbance Atlas (EFDA) (Viana-Soto and Senf, 2024; see Table 3 for a detailed summary). The resolution of all layers is 30-m, containing information from 1985 to 2023 (in the current version 2.11). The data is distributed at the country level using the ETRS89 coordinate reference system and the Lambert Azimuthal Equal-Area projection (ETRS89-extended / LAEA Europe; EPSG:3035) and can be downloaded from (https://doi.org/10.5281/zenodo.13333034).

Table 3. Summary layers of the European Forest Disturbance Atlas

	Name	Valid range	Description
Forest land use mask	forest_mask_{country}	1	Forest land use mask
Annual disturbance	annual_disturbances_1985_2023_{country}	(0, 1)	Stack of annual disturbances indicating undisturbed (0) and disturbed (1)
Disturbance probability	disturbance_probability_1985_2023_{country}	(0, 100)	Stack of annual disturbance probabilities within forest areas
Latest disturbance	latest_disturbance_{country}	(1985, 2023)	Indicates the year of the most recent disturbance
Greatest disturbance	greatest_disturbance_{country}	(1985, 2023)	Indicates the year of the highest disturbance severity (greatest spectral change)
Number of disturbances	number_disturbances_{country}	Categorical (1, 2, 3, 4)	Indicates the number of disturbance events within the time-series (1, 2, 3, or more than 3 events, i.e. 4)
Disturbance severity	disturbance_severity_1985_2023_{country}	(-10,000, 10,000)	Stack of spectral change in NBR for disturbance patches ($t - t_{-1}$).
Disturbance agent	disturbance_agent_1985_2023_{country}	Categorical (1, 2, 3)	Annual classification of disturbance agents (1- wind/bark beetle, 2- fire, 3- harvest).
Aggregated disturbance agent	disturbance_agent_aggregated_{country}	Categorical (1, 2, 3, 4)	Aggregated layer of agents that summarises the dominant agent within the time-series. In those cases where a pixel has been disturbed more than once and by multiple agents, the class mixed (4) is assigned.

3. Results

3.1. Map products in the EFDA

Our newly created Forest Disturbance Atlas for Europe provides a set of variables at 30-m describing forest disturbances annually since 1985 (Figure 5). By mapping disturbances annually, we capture multiple disturbance events to obtain direct

information on the number of disturbances, the latest disturbance (most recent disturbance event), and the greatest disturbance (event with the greatest spectral change). The annual disturbance maps are coupled with the estimated annual disturbance probabilities from Random Forest as a proxy of uncertainty on disturbance detection (Figure B1 appendix). Maps are constrained to our forest land use mask, which includes areas that have been forest at some point within the time series and thus avoids masking recently disturbed areas.

Figure 5 shows a Europe-wide overview of the area affected by disturbances over the last four decades. The individual layers show the ability of our atlas to precisely retrieve disturbance characteristics across different disturbance regimes, such as a recent bark beetle outbreak interspersed with harvest activities in the Thuringian Forest in Germany (Figure 5a~~.1~~), interactions between different agents in an intensively managed forest plantation in the Gascony region in France (Figure 5~~.2~~b), where a windstorm was captured in 1990 and a recent fire occurred in 2023, as well as recurrent fires in planted forests in central Portugal (Figure 5~~.3~~c).

Based on the annual disturbance estimates (Figure 6), we quantified a total forest disturbed area of 439,000 km^2 (22% of the total forest area) that increases to 610,000 km^2 when accounting for multiple disturbance events (i.e. considering area disturbed in multiple years, such as reburns or multiple harvests). From those disturbed areas, 72% correspond to areas with one disturbance event while 18.9% (115,000 km^2) have two disturbance events, and 9.1% (55,000 km^2) have three or more disturbance events. That is, a total of 28% of all pixels disturbed in Europe in the past four decades had multiple disturbance events. These multiple disturbances mostly occur in southern Europe (e.g. Portugal, Spain), where multiple fires occurred interspersed with harvesting activities, as well as in regions characterized by short-rotation plantation systems, e.g. the south of France, Hungary, Poland or Sweden, with harvests return periods of 15-20 years. Planned disturbances caused by human land use (harvest) caused 79.2% of the total disturbed area and the natural agents were responsible of 20.8% of the disturbances found (12% from wind and bark beetle outbreaks and 8.8% from wildfires).

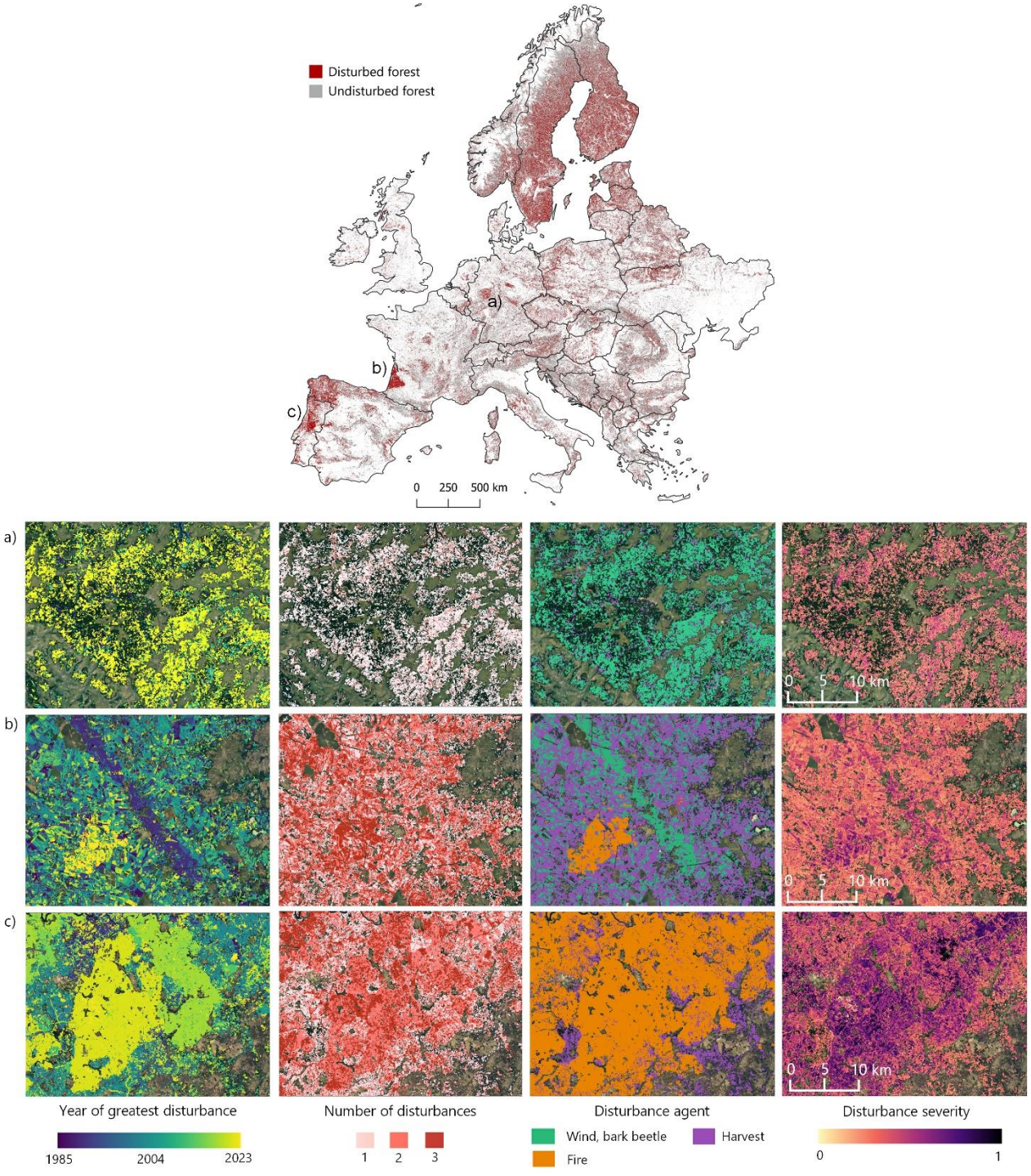

Figure 5. Forest disturbances in Europe (1985-2023). Details show (a) bark beetle outbreaks in central Germany; (b) a combination of a windstorm event and a recent fire in a managed forest plantation in Gascony (France); and (c) recurrent fire disturbances in central Portugal.

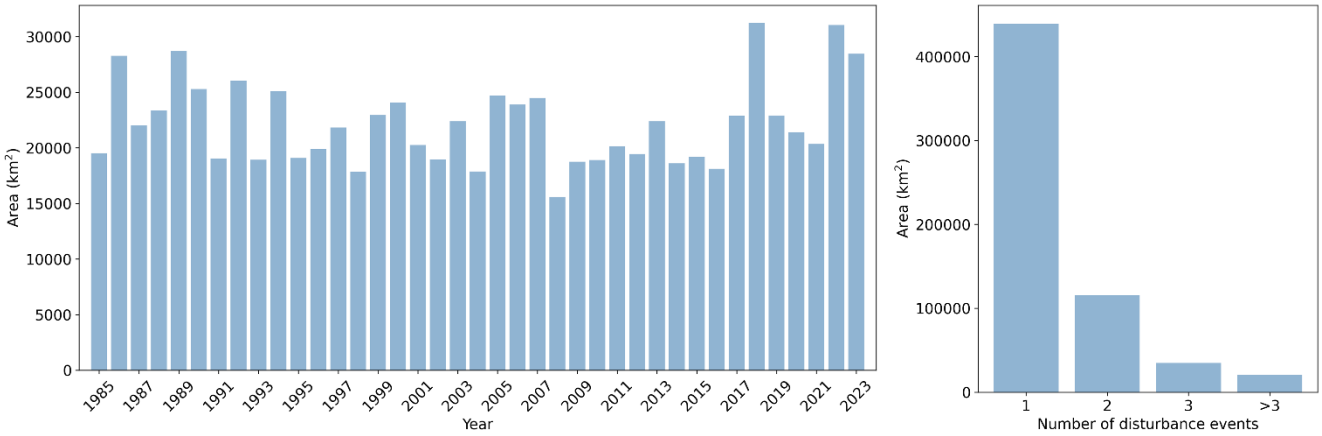

Figure 6. Number of hectares disturbed per year (a) and area disturbed per number of events (b)

3.2. Validation~~Accuracies and uncertainties~~

The assessment of the land use mask, discriminating between non-forest and forest land use, yielded high accuracies with an overall F1-score of 0.92, with F1-scores of 0.93 for non-forest and 0.91 for forest land use, respectively (Table 4). Commission and omission errors were thus overall low (<10%) and well balanced, indicating that on average 7.5% of the pixels in the land use mask will be wrongly classified. Further, comparison of the estimated forest area at national level with forest land use area from FAOSTATS showed a high agreement (R^2 = 0.98; MAE = 6,019km^2, 16.9%; Figure 7), with a slight tendency of overestimating forest area.

Table 4. Confusion matrix of the forest land use map

	Reference data				
	Non-forest	Forest	N	Commission errors (%)	Confidence intervals
Non-forest	1025	61	1086	**5.6**	[90.1 - 99.9]
Forest	91	851	942	**9.7**	[87.1 - 93.9]
N	1116	912			
Omission errors (%)	**8.2**	**6.7**			
Confidence intervals	[87.9 - 94.8]	[89.9 - 98.2]			
F1 score	**0.93**	**0.91**	Overall accuracy = 92.5 % | Overall error = 7.5 %		

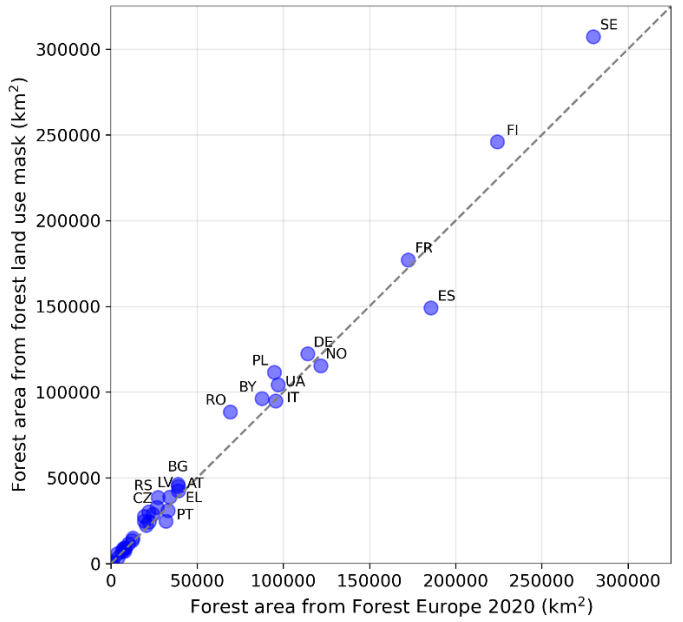

Figure 7. Forest area according to FAOSTATS 2020 versus forest land use estimated for the series 1985-2023.

Map accuracies of the disturbance classification showed an overall F1-score of 0.89, with F1-scores of 0.99 for undisturbed and 0.80 for disturbed pixels (Table 5). Accuracies were thus less balanced between both classes, with very low commission/omission errors (<1%) for the undisturbed class (i.e. the map rarely misses or falsely classifies something as undisturbed), but higher commission and omission errors for the disturbed class (17.3% and 22.5%, respectively). That is, for 17% of all pixels classified as disturbance the classification will be wrong, whereas 23% of true disturbances will be missed in our map. Those numbers changed significantly when only considering reference points interpreted as stand-replacing disturbances in the reference data (Table B1 appendix), with a substantially reduced omission error (14.2% vs. 22.5%) and a slightly increased commission error (22.7% vs. 17.3%). The omission error of our map is thus driven by low-intensity disturbances that remove the tree canopy only partially. We found significant variation in accuracies among regions, with higher commission error in Northern Europe compared to Central and southern Europe, whereas omission was lower in Northern Europe compared to Central and Southern Europe (Table 6). In Northern Europe, it is thus more likely to randomly select a pixel falsely detected as disturbance but less likely that a true disturbance is missed, while in Central and Southern Europe it is more likely to miss a true disturbance than falsely identifying a pixel as disturbed. In the temporal domain we found overall high fluctuation between years, yet an overall decreasing trend in commission error but no clear trend in omission error (Figure 8). That is, disturbances mapped before the year 2000 will have an 19.5% chance of being falsely classified as disturbance, whereas commission substantially decreases to 10.6% after the year 2000 (Table B2 appendix). The high commission error prior to 2000 was driven significantly by the very early years of our time series (<1990), where commission error was on average 22.5% (compared to 16.4% between 1990 and 1999), likely due to higher noise in the underlying data.

Omission errors showed a less clear pattern, with also higher omission rates in the 80s (23.3%), likely due to lower image availability, but less pronounced differences before/after the year 2000 (22.5% and 20.5%, respectively). Finally, we found high agreement between estimated and manually interpreted disturbance years (R^2 =0.73; Figure 9), with a mean absolute error of 1.91 years.

Table 5. Confusion matrix of disturbance detection assessment

	Reference data				
	Undisturbed	Disturbed	N	Commission errors (%)	Confidence intervals
Undisturbed	83206	220	83426	**0.26**	[99.70 - 99.89]
Disturbed	158	756	914	**17.29**	[77.30 - 87.78]
N	83364	976			
Omission errors (%)	**0.18**	**22.54**			
Confidence intervals	[99.65 - 99.83]	[71.98 - 82.27]			
F1 score	**0.99**	**0.80**	Overall accuracy = 89.9 % | Overall error = 10.1 %		

Table 6. Errors in disturbance detection per region

	North		**Central**		**South**	
	Commission errors (%)	Omission errors (%)	Commission errors (%)	Omission errors (%)	Commission errors (%)	Omission errors (%)
Undisturbed	0.14	0.2	0.2	0.1	0.13	0.1
Disturbed	23.32	18.1	13.62	26.96	16.99	22.97

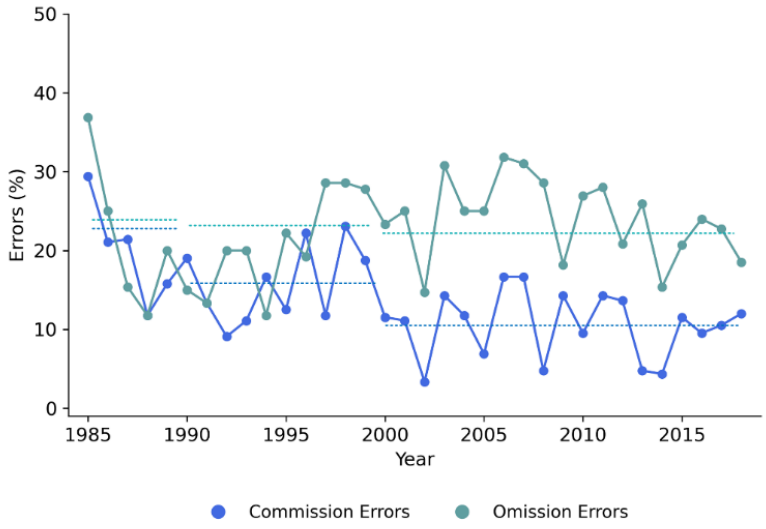

Figure 8. Omission and commission errors per year. Dashed horizontal lines indicate the averages per period 1985-1989, 1990-1999, 2000-2018.

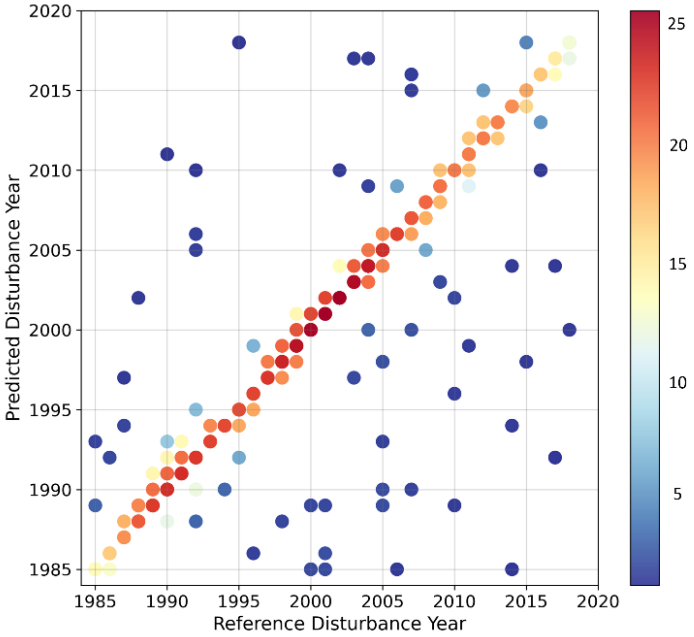

Figure 9. Validation of the disturbance year. Estimated disturbance year versus manually interpreted year of disturbance for independent reference pixels (colour bar indicates the number of points)

The model predicting the disturbance agent performed well, having an overall error rate of 14.1 %, with a commission error rate (false occurrences) of 10.5% for bark beetle/windstorm disturbances, 5.7% for fire disturbances and 17.4% for harvest (Table 7). The omission error rate (i.e. model missed a true occurrences) was 19.1% for bark beetle/windstorm disturbances, 25.5% for fire-related disturbances and 8.7% for harvest. We note again that the accuracies reported here are model accuracies and not map accuracies derived from an independent sample.

Table 7. Confusion matrix of disturbance agent model assessment

	Reference data				
	Bark Beetle /Windstorms	Fire	Harvest	N	Commission errors (%)
Bark Beetle /Windstorms	9066	48	1019	10133	10.53
Fire	3	831	47	881	5.68
Harvest	2130	236	11248	13614	17.38
N	11199	1115	12314		
Omission errors (%)	19.05	25.47	8.66		
					Overall accuracy = 85.9% | Overall error = 14.1 %

3.3. Comparison to other datasets

Comparison of EFDA disturbances maps with available datasets for Europe (Hansen et al., 2013; Senf and Seidl, 2021a; Turubanova et al., 2023) revealed differences in annual estimates, but also showed similarities in increasing disturbance area since 2001 (Figure 10). Overall, EFDA's average annual disturbance area (19,544 km^2 per year) was 30.2% higher than estimates in Turubanova et al. (2023) (13,631 km^2 per year), 33.2% higher than estimates in Senf and Seidl (2021a) (13,038 km^2 per year), and 42.6% higher than estimates in Hansen et al., (2013) (11,207 km^2 per year). Using EFDA's latest disturbance map (average annual disturbance area of 14,756 km^2) instead of the annual disturbance maps, however, improved agreement with the other maps significantly: 7.6% for Turubanova et al. (2023), 11.6% for Senf and Seidl (2021a) and 24% for Hansen et al. (2013), indicating that multiple disturbances can increase disturbance estimates substantially.

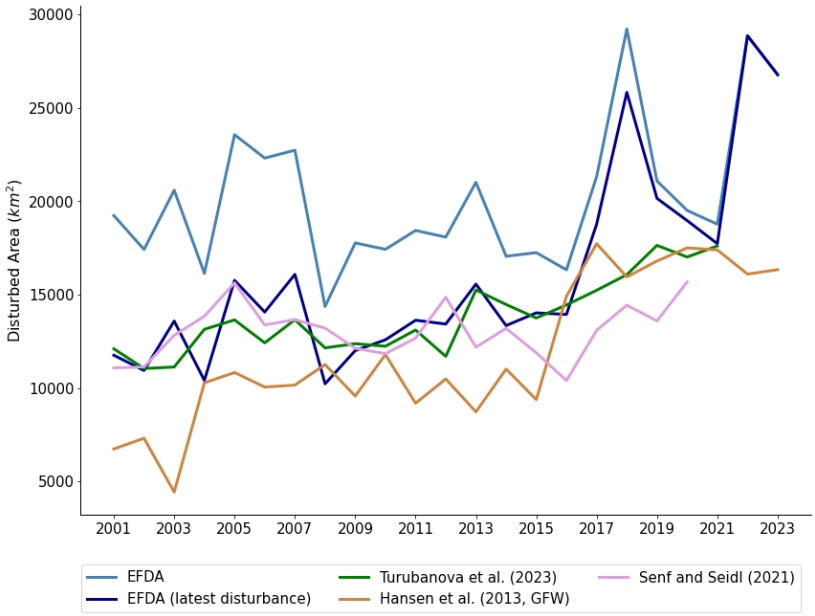

Figure 10. Annual disturbed area estimates from current available datasets for Europe.

4. Discussion

We here presented the European forest disturbance atlas (EFDA), providing spatially explicit information on disturbances since 1985 and demonstrating the importance of long time series for understanding disturbance change, disturbance regimes and disturbance interactions. While there are already several disturbance products for Europe (Senf and Seidl, 2021a; Turubanova et al., 2023), our new dataset moves beyond existing products in at least three important ways: First, annual disturbance mapping enables to capture multiple disturbance events, providing direct information on disturbance frequencies and temporal interactions. Multiple disturbance information is often not assessed or simplified to the greatest or latest

disturbance of the analysis period. Without capturing disturbances on an annual basis, however, we lose valuable information on forest dynamics (Buma, 2015; Hermosilla et al., 2019), such as disturbance return times (Pugh et al., 2019), and might lead to underestimation of total disturbance area (see Figure 10). We found, for example, return times of 15-20 years in recurrent fires in the Mediterranean or in short rotation plantations across Europe (e.g. Hungary, Sweden, Netherlands), and further temporal interactions between harvest and wind disturbances in the Gascony area in France (i.e. wind disturbance following a harvest event). Including multiple disturbances was thus an important improvement over past map products available for Europe. Second, the long-time frame of our map products offers a baseline for understanding more recently observed changes and for quantifying trends over time. Furthermore, our workflow is designed to be operationally updated when new data arrives and therefore enables to create up-to-date maps annually after the summer season. Third, our approach is consistently applicable over all European forests with variable forest types and forest disturbances. It thus is likely to be adoptable and replicable in other regions. To facilitate user uptake and reproducibility, we provide a full open access framework that can be implemented on any computer system, independent of commercial cloud environments, data providers or software tools. The European Forest Disturbance Atlas thus contributes to a future operational forest monitoring envisioned for Europe.

One of the aims of this paper was to provide a full characterization of map ~~uncertainties~~accuracies. Compared to the first pan-European disturbance product developed by Senf and Seidl (2021a), which reported a commission error of 17.1% and an omission error of 36.9% for detecting disturbances, we reduced omission errors considerably (22.5%) while maintaining low commission errors (17%). That is, the EFDA detects more true disturbances compared to the past state-of-the-art product, while making similar errors in falsely detecting disturbances. Disturbance areas derived from Senf and Seidl (2021a) are thus likely conservative estimates that underestimate true disturbance area (Figure 10). A similar improvement was found in the timing of disturbances, with a mean absolute error of 3 years for Senf and Seidl (2021a) compared to 1.9 years for our map, indicating that fewer disturbances are attributed to a wrong year compared to manually interpreted data. The disturbance detection accuracies found here are further consistent with more local approaches implemented in Europe, such as Francini et al. (2021), who reported omission/commission errors of 27% and 30% for clear-cut mapping in Italy with the 3I3D algorithm; or recently developed disturbance maps for the European Alps (Morresi et al., 2024), with omission/commission errors of 16.9% and 16.5%, and for continental Spain (Miguel et al., 2024), with omission/commission errors of 12.4% and 18%, respectively. Our map was of slightly lower accuracy than a very recent pan-European forest disturbance map developed by Turubanova et al. (2023), with omission and commission errors of ~19% and ~7%, but their map only covers disturbances since 2001. Comparing our map accuracies to Turubanova et al. (2023) for the same period yields approximately similar accuracies between both map products (see Figure 8). Finally, our forest land use mask yielded high accuracies and the forest area estimated per country aligned well with estimates provided by FOREST EUROPE (2020). Remaining differences can be explained by the different temporal reporting periods, as FOREST EUROPE reports the forest area in 2020 but we provide a multitemporal land use definition, comprising all areas that have been forest land use at some point since 1985. Our forest land use map is also distinctly different from recent tree cover products (Liu et al., 2023; Turubanova et al., 2023), as it includes

recently disturbed areas that might be temporally unstocked but return to closed canopy forests in the near future (Mandl et al., 2024) and thus meet our forest land use definition. Using static tree cover maps would mask out those areas based on the (arbitrary) year they were created for. We thus move away from a static forest cover map to a forest land use map that reflects the spatial and temporal dynamics of forests (Chazdon et al., 2016).

Beyond accuracies reported from different datasets, dissimilarities were found in annual disturbed area estimates from different maps, with the EFDA leading to +7.6% to up to +42% higher estimates in average annual disturbance area. Several factors are likely responsible for those stark differences, including different map accuracies, disturbance detection logics (i.e. definition of disturbance and model calibration), and forest mask definitions. First, the EFDA has a lower omission error than previous products (see previous paragraph), which must lead to a higher disturbance area, because fewer disturbances are missed in our map than in previous maps. This becomes especially evident when comparing maps tailored for Europe (Senf and Seidl, 2021a; Turubanova et al., 2023) to global products (Hansen et al., 2013), who substantially underestimate disturbed area. Second, the EFDA allows for multiple disturbances, which can increase disturbance area in comparison to summary products that only allow for one disturbance per time series (i.e. Senf and Seidl 2021a). We show this impressively in Figure 10, where our annual disturbance estimate is substantially higher than the annual summarized to their latest disturbance. Accounting for multiple disturbances (which we estimate for 28% of all pixels) thus makes a difference in total disturbance area estimates, because more recent/higher severity disturbances can mask out older/less severe disturbances. We found this to be especially prominent in systems dominated by fire, where areas that have burned in the mid 1990s or mid 2000s burned again in the most recent years (e.g. Portugal); or where plantation forests that had multiple harvests in the past now burned in more recent years (e.g. France). Third, forest area definitions vary widely between map products and thus are likely a main factor explaining differences between disturbance estimates, especially comparing our product to Turubanova et al. (2023) and Hansen (2013). Both apply a very strict tree cover definition that will mask out any pixels that have ~~n't~~ not met the definition. This can lead to disturbances patches being fragmented into several smaller disturbances. That is, while all map products detect the disturbance event, the actual area disturbed can vary quite significantly. Strict tree cover definitions, especially in terms of tree height, can also lead to missing multiple disturbances (i.e. reburning fires), which might also explain some of the differences to our annual disturbance maps (see Figure 11a). Further, image availability and observation gaps (e.g. ETM+ SCL-off problems) can also contribute to missing disturbed areas in large disturbance patches. One stark difference between EFDA and the other datasets could be detected in 2018 and 2022 (Figure 10), which was driven by commission errors in northern regions (see Table 6, Figure 11c). Both years were particularly dry in Fenno-Scandinavia and Central Europe (Knutzen et al., 2025), leading to strong spectral differences, especially in wetland areas (Figure 11c). Yet, the disturbance peak in 2018 detected in the EFDA coincides with a peak of natural disturbance activity reported earlier (Patacca et al., 2023), attributed to large-scale bark beetle outbreaks in Central Europe (see Figure 11b). Discrepancies between disturbance maps have also been reported for other regions (Cohen et al., 2017), with even stronger disagreement. It is therefore necessary to cautiously analyse and understand the methodological nuances of the different approaches to consider how errors might influence use in a variety of contexts.

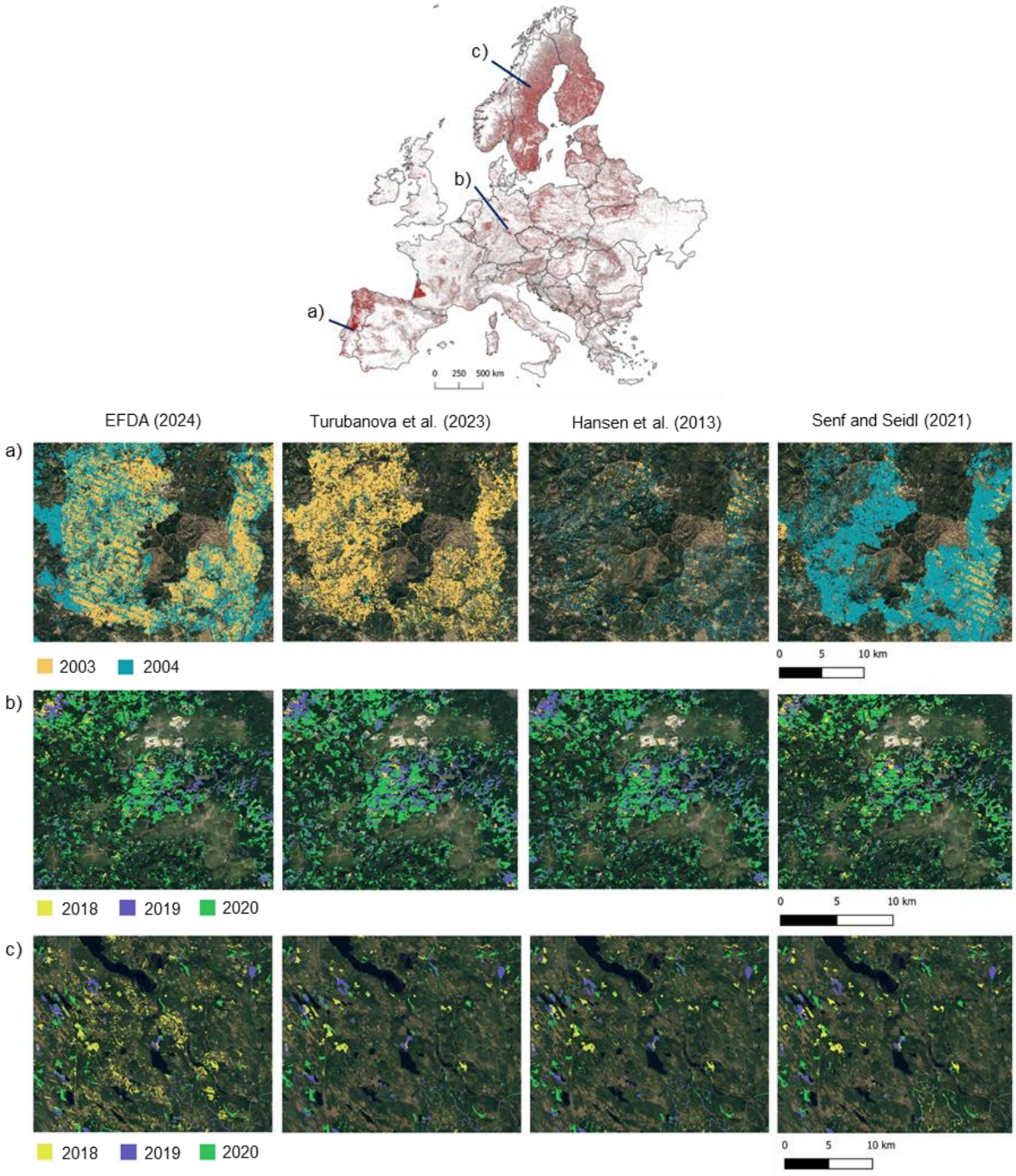

Figure 11. Examples of disturbance maps from different datasets for (a) fires in Central Portugal, (b) bark beetle outbreaks in Central Germany, (c) harvests in northern Sweden.

Despite the good accuracies compared to past and other map products, there are several limitations and possible sources of uncertainties that should be considered when using the EFDA. The higher omission error for the disturbed class and wider confidence intervals indicates a possible limitation of our approach when mapping low severity disturbances that do not produce a clear opening of the canopy (e.g. canopy thinning). The effect of such non-stand replacing disturbances is clearly seen when redoing the accuracy assessment without them, which nearly halved the omission error (Table B1 appendix). Non-stand replacing disturbances area quite widespread in central and southern Europe, leading to higher omission errors in those regions compared to northern Europe mostly characterized by clearcut harvesting. In northern Europe, however, a higher frequency of missing data and noise (i.e. remaining clouds, difficult illumination conditions, short summer season) led to higher commission errors in comparison to central and southern Europe, where data availability was overall higher (see Figure 2b). We further found that omission errors were caused by a delayed detection of disturbances (i.e. disturbances detected one year after the reference). The detection of disturbances with a delay of one year is a common problem when working with annual summer composites, where disturbances can occur in the same year but after the compositing date (i.e. a pixel is selected from August, but the disturbance occurs in November and will thus only be detected the next summer). Finally, the use of a minimum mapping unit may contribute to the omission of small-scale disturbances < 0.27 ha, but reduces false positives from individual isolated pixels (Reinosch et al., 2024). We thus argue that the loss of information imposed by the minimum mapping unit outweighs the potential error by included many small-scale disturbances with high errors. The application of a minimum mapping unit is also a common practice to facilitate the integration with different data sources such as national forest inventories (Wulder et al., 2024) or national land use products (Gómez, et al., 2019). The temporal validation revealed variability in accuracy over the time series, with the 1980's and 1990s having considerably lower accuracies (especially in terms of commission error) than disturbances detected after 2000s (Figure 8, Table B2 Appendix). This result highlights challenges with reliability estimating disturbance trends from remote sensing data (see Olofsson et al., 2014 for an in-depts discussion), as trends derived from disturbance maps with variable accuracy will be biased (Palahí et al., 2021). Quantification of disturbances and trends should thus be based on a manually interpreted sample or based on models taking in to account the variable accuracies over time (Francini et al., 2022; Olofsson et al., 2014). Finally, despite careful processing and checking, there will be remaining errors in the underlying remote sensing data and specific regions and years will have large errors resulting from noise. For example, some peaks of higher omission errors displayed in Figure 8 coincide with years of higher percentage of no-data pixels as for example in the 80s, 1998, 2008 or 2012 (Figure A2 - appendix). This limitation is intrinsic to the data used for producing the EFDA, but so far there is no other consistent alternative to provide spatially explicit and consistent information for monitoring Europe's forest over time.

We provide an agent attribution layer based on a previous established model (Seidl and Senf, 2024), complementing the disturbance layers of the EFDA described in this study. Although comparison of estimates with existing databases for fire and storms in Senf and Seidl (2021b) and salvage logging in Seidl and Senf (2024) showed high agreement of the attribution model with external datasets, an independent validation sample on the actual occurrence of disturbance agents is still missing for

robust reporting of uncertainties. According to the random forest variable importance (see Figure A6), landscape pulse dynamics (see table 2) and patch size were most important for disentangling disturbance agents, likely because they typically occur in clusters and are characterized by larger, more complex patch shapes. In contrast, harvest tend to be more regular in space and time (Senf and Seidl, 2021b). ~~Further~~However, the fact that management superimposes most natural disturbances though salvage logging makes it difficult to disentangle the root cause of disturbance. This is especially true when natural disturbances are salvage logged, because the annual resolution of the EFDA does not allow to disentangle the initial natural disturbance and the subsequent salvage logging. That is, most of the natural disturbance mapped in the EFDA will be a combination of an inciting natural factor (bark beetle or wind disturbance) and subsequent salvage logging (Seidl and Senf, 2024). We also miss less prevalent natural disturbance agents in our attribution map (Stahl et al., 2023), such as drought and more gradual non-stand replacing disturbances that can also impact on forests globally (Coops et al., 2020; Hammond et al., 2022). The agent attribution provided in the EFDA should thus be taken with caution, as reliable estimates of map accuracies are absent and making causal claims on importance of natural disturbances remains challenging (despite our estimate of 20.8% natural disturbances matching well with Patacca et al. (2023). Novel data collected across Europe might help with overcoming challenges with agent attribution (Forzieri et al., 2020, 2023; Patacca et al., 2023), but most data does not cover the 80s and 90s, which are especially important for improving map accuracy and quality. Further research should thus increasingly focus on generating reference data that can be used for remote sensing applications (e.g. Franquesa et al., 2020; Senf, 2019), and we urge authors to make their reference data openly available, ultimately leading to a better understanding of forest change across Europe.

5. Conclusion

There is high need for an operational forests monitoring system at European scale and our newly developed disturbance atlas (EFDA) constitutes a first step in this direction by producing disturbance information in a standardised way, with consistent quality across all of Europe's forest. Our approach further relies on open-source data and tools and is implemented in an open-access framework, which allows full reproducibility and easy updating into the future and thus paves the road for operationalisation. Our data covers already 40 years of forest disturbance dynamics, constituting the longest remote sensing-based disturbance products available at continental scale today. Covering such long-time series allows for a better characterisation of disturbance regimes, requiring several decades of data to reliably quantify underlying distributions (Maroschek et al., 2024), as well as they can help to improve disturbance modelling by providing empirical data on disturbance occurrence (e.g. Grünig et al., 2022). Hence, the EFDA will improve our understanding of European forest disturbance dynamics beyond simple monitoring forest disturbances.

Code and data availability

The European Forest Disturbance Atlas data is freely accessible under https://doi.org/10.5281/zenodo.13333034 (Viana-Soto and Senf, 2024) and summary layers are accessible through Google Earth Engine in ee.Assets.latest_disturbance_v211, ee.Assets.number_disturbances_v211, ee.Assets.disturbance_agent_v211. The maps can be also explored online: https://albaviana.users.earthengine.app/view/european-forest-disturbance-map. The code used for processing the Landsat data using FORCE is available in https://github.com/davidfrantz/force. The code used for the subsequent processing steps is available in https://github.com/albaviana/European-Forest-Disturbance-Atlas.

Author contributions

A.V.S. and C.S. designed the research. C.S. compiled the reference data. A.V.S. performed all computations and analyses. A.V.S. and C.S. wrote the manuscript.

Competing interests

The contact author has declared that none of the authors has any competing interests.

Disclaimer

This research reflects only the authors' view, and the European Commission is not responsible for any use that may be made of the information it contains. Publisher's note: Copernicus Publications remains neutral with regard to jurisdictional claims in published maps and institutional affiliations.

Acknowledgements

A.V.S. and C.S. acknowledge funding from ForestPaths project (Co-designing Holistic Forest-based Policy Pathways for Climate Change Mitigation, ID No 101056755) funded from the European Union's Horizon Europe Research and Innovation Programme and from AI4Forest project funded through the German Federal Ministry of Education and Research (BMBF). We thank David Franzt (Trier University) for developing, maintaining and making the code of FORCE open source. We thank Michael Reuss for facilitating the gap-filling process.

Appendix A

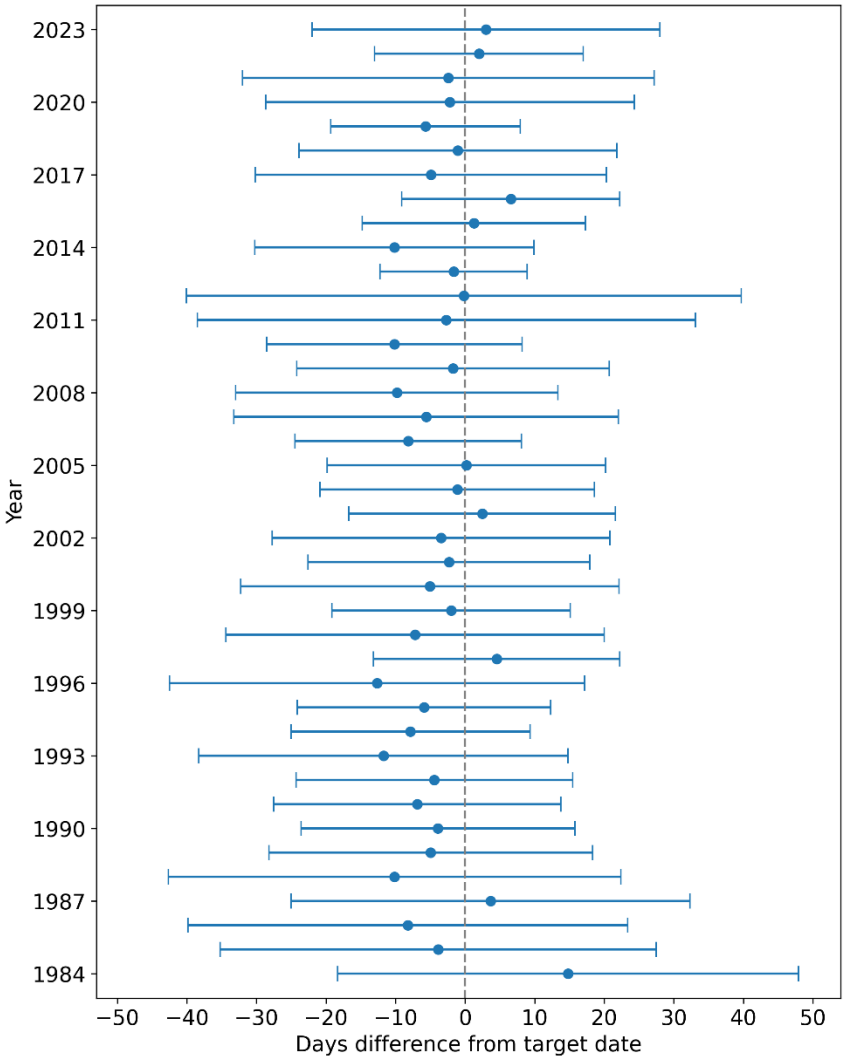

Figure A1. Days difference from target date (1st of August) per year (Mean +- Standard Deviation).

565

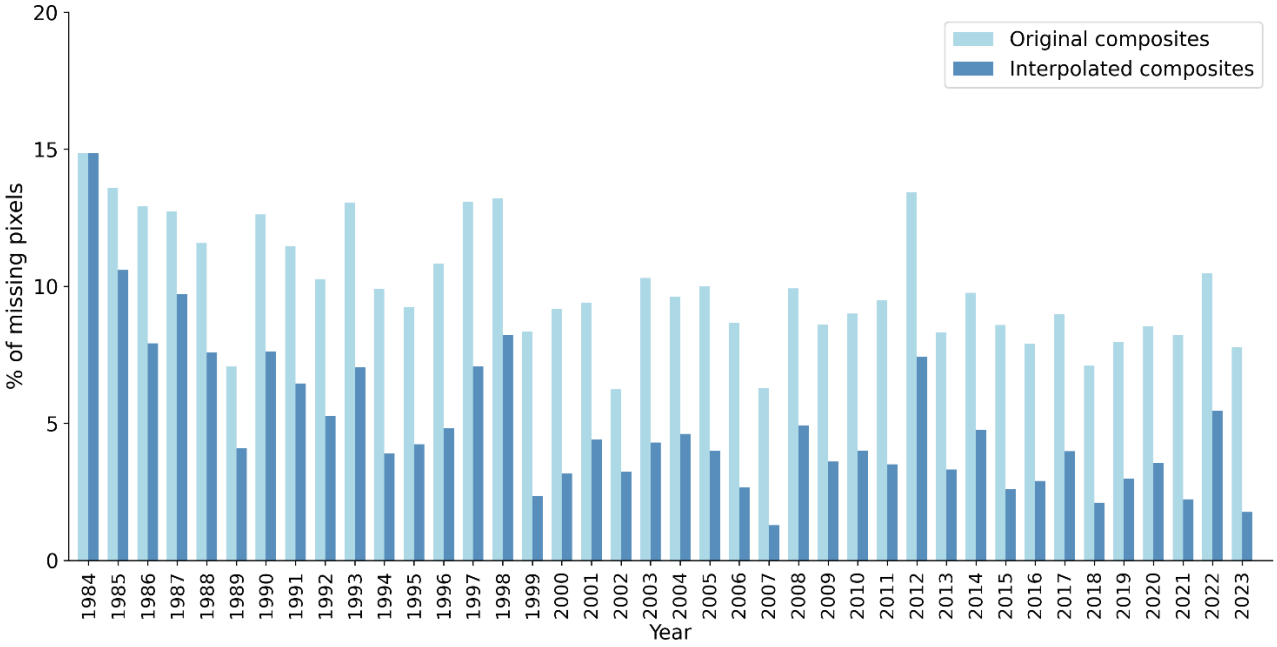

Figure A2. Annual percentage of no-data pixels for best available pixel composites and after linear gap-filling interpolation.

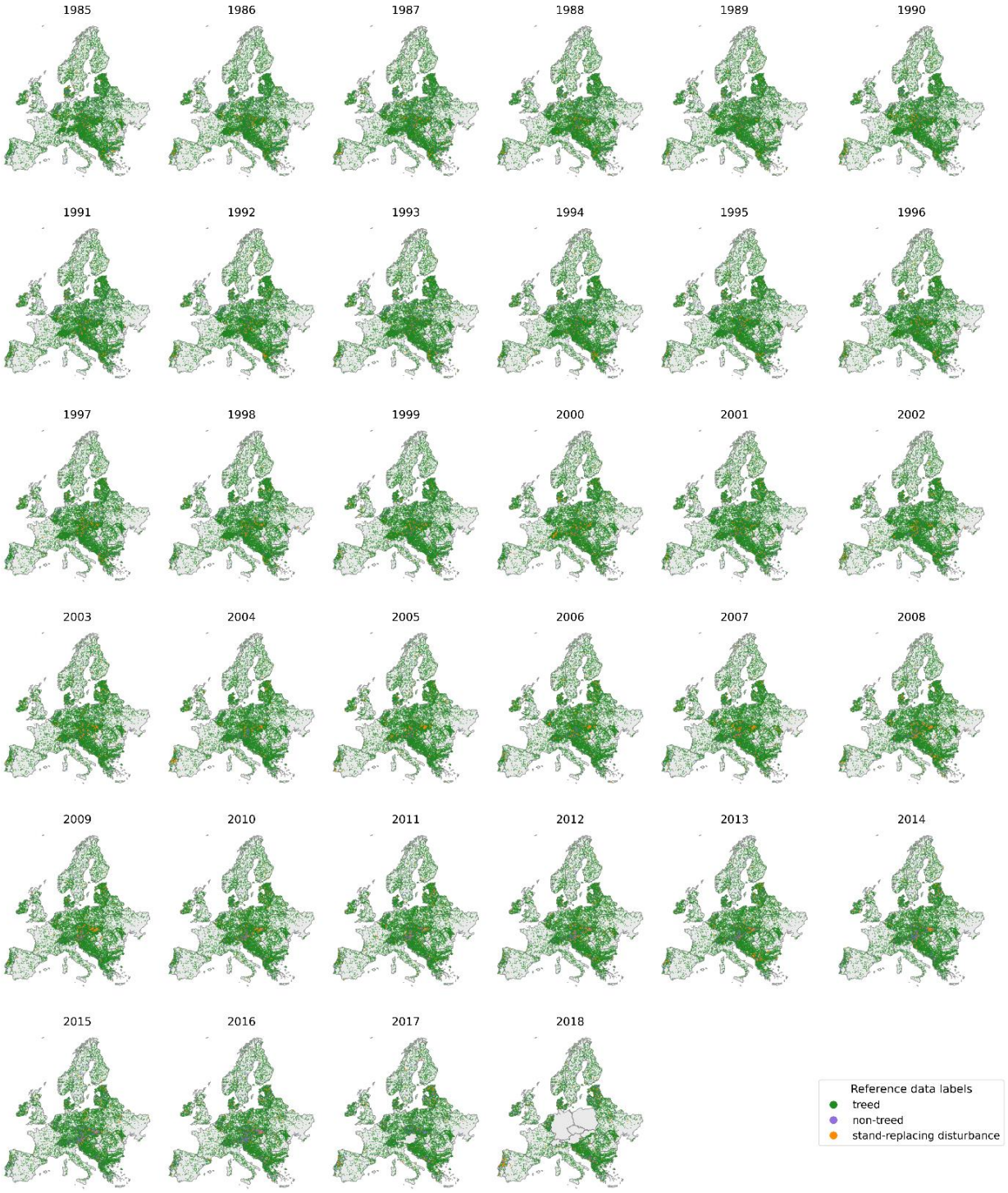

Figure A3. Maps of annual reference data within forests for disturbance and undisturbed (treed and non-treed).

Table A1: Spectral indices and Tasseled Cap components equations for Landsat

Name	Equation	Reference
Normalized Burn Ratio (NBR)	$\frac{(NIR - SWIR2)}{(NIR + SWIR2)}$	(García and Caselles, 1991)
Normalized Difference Vegetation Index (NDVI)	$\frac{(NIR - Red)}{(NIR + Red)}$	(Tucker, 1979)
Tasseled Cap Brightness (TCB)	Blue × 0.3029 + Green × 0.2786 + Red × 0.4733 + NIR × 0.5599 + SWIR1 × 0.508 + SWIR2 × 0.1872	(Baig et al., 2014)
Tasseled Cap Greenness (TCG)	Blue × (-0.2941) + Green × (-0.243) + Red × (-0.5424) + NIR × 0.7276 + SWIR1 × 0.0713 + SWIR2 × (-0.1608)	
Tasseled Cap Wetness (TCW)	Blue × 0.1511 + Green × 0.1973 +Red × 0.3283 + NIR × 0.3407 + SWIR1 × (-0.7117) + SWIR2 × (-0.4559)	
Disturbance Index (DIn)	$TCBn - (TCGn + TCWn)$ *where n indicates values are normalized*	(Healey et al., 2005)

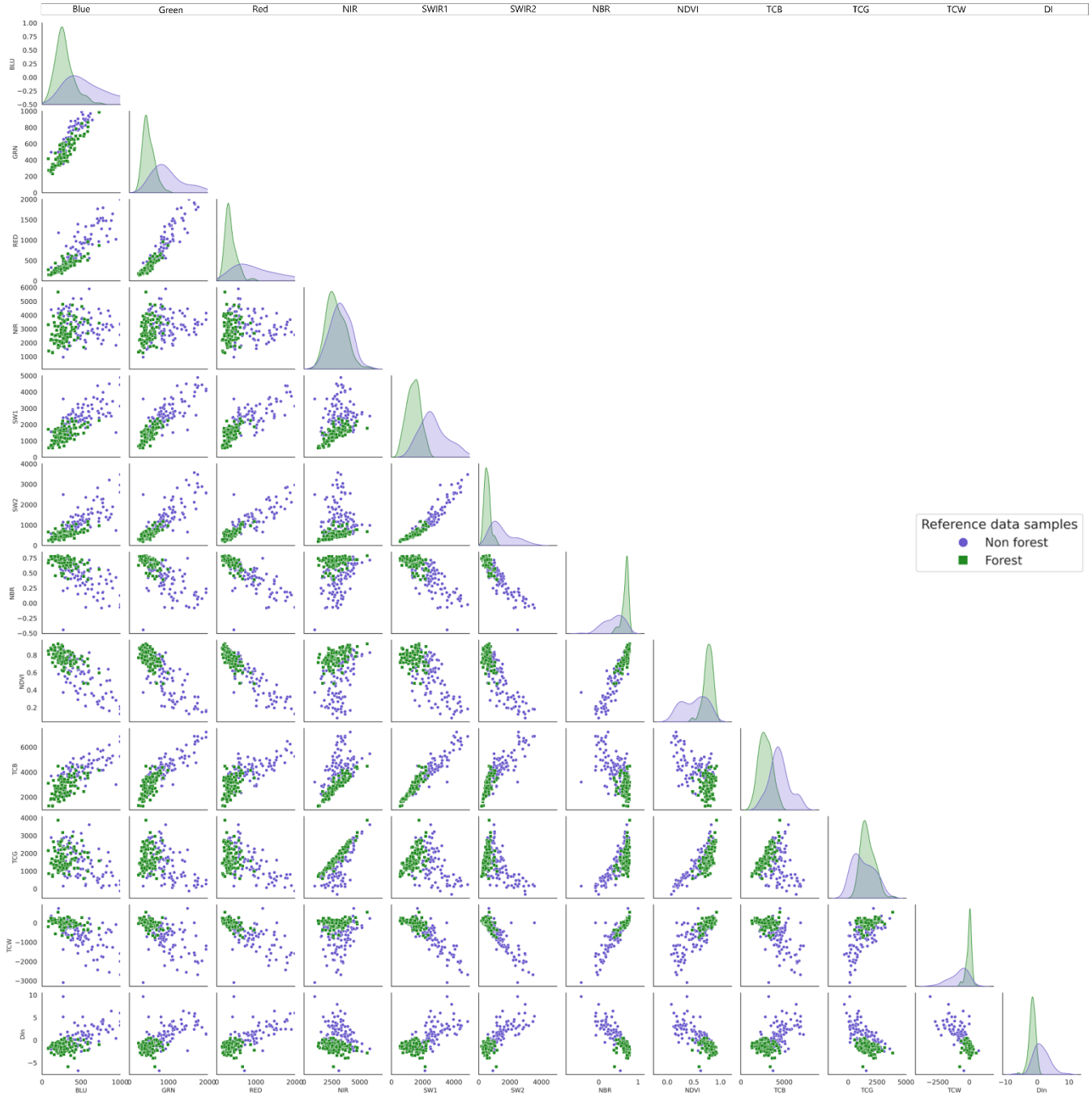

590 **Figure A4. Feature space of spectral bands and indices for forest and non-forest reference samples.**

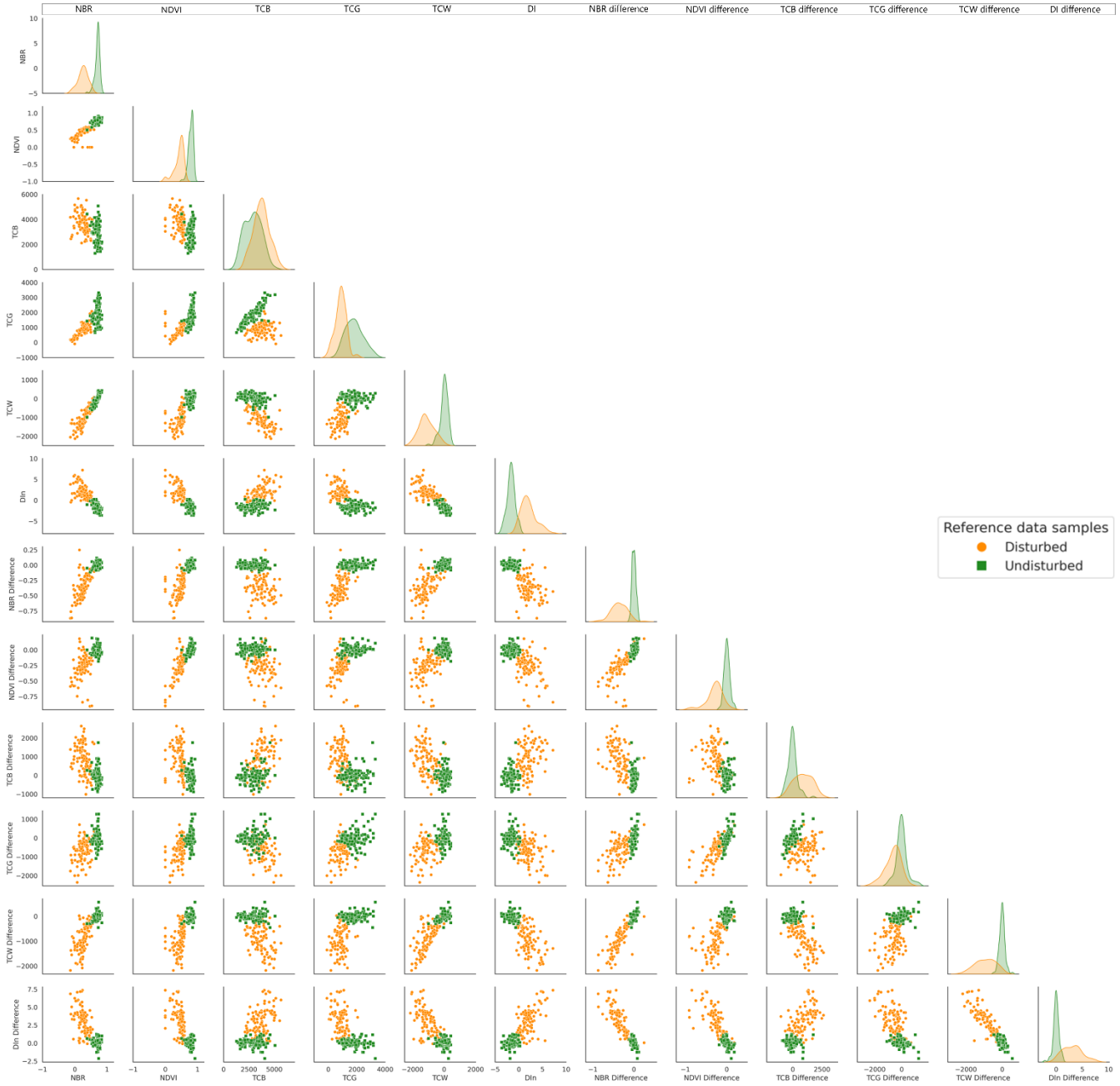

Figure A5. Feature space of spectral indices for disturbed and undisturbed reference samples.

595

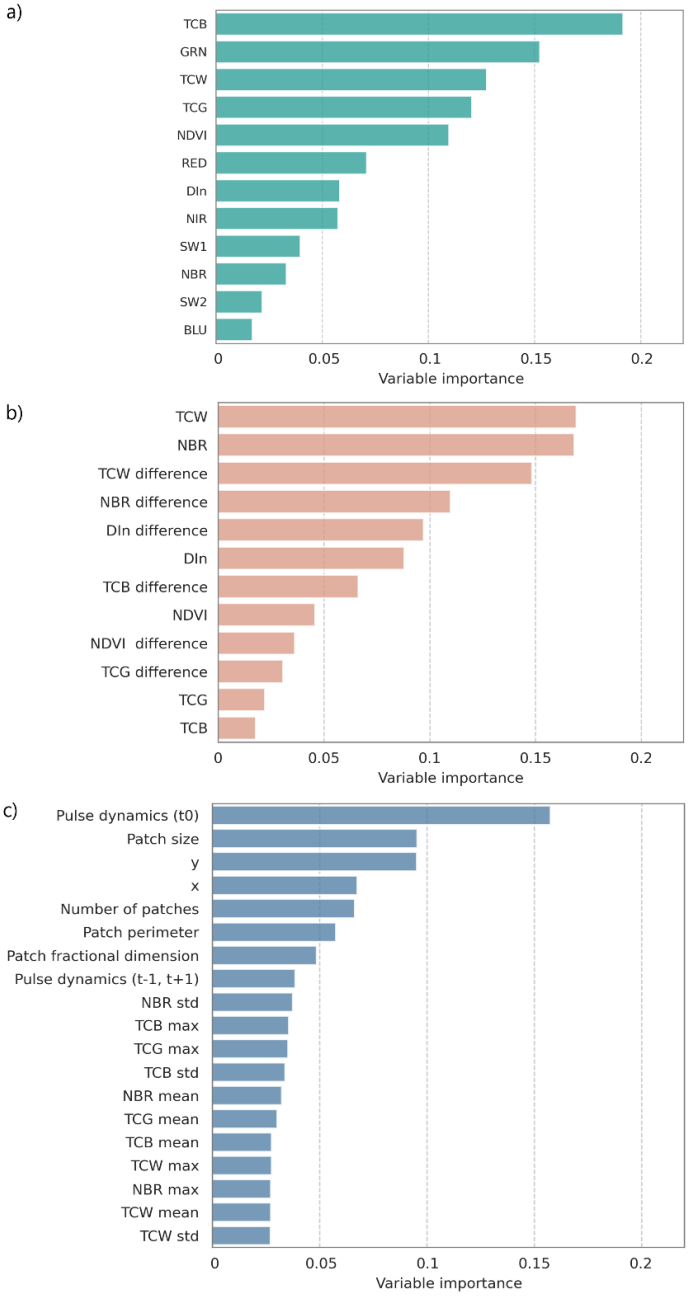

Figure A6. Variable importance (as returned by the random forest algorithm) for a) forest land use classification, b) disturbance-no disturbance classification, and c) disturbance agent attribution model. Higher values indicate higher importance for discrimination.

Appendix B

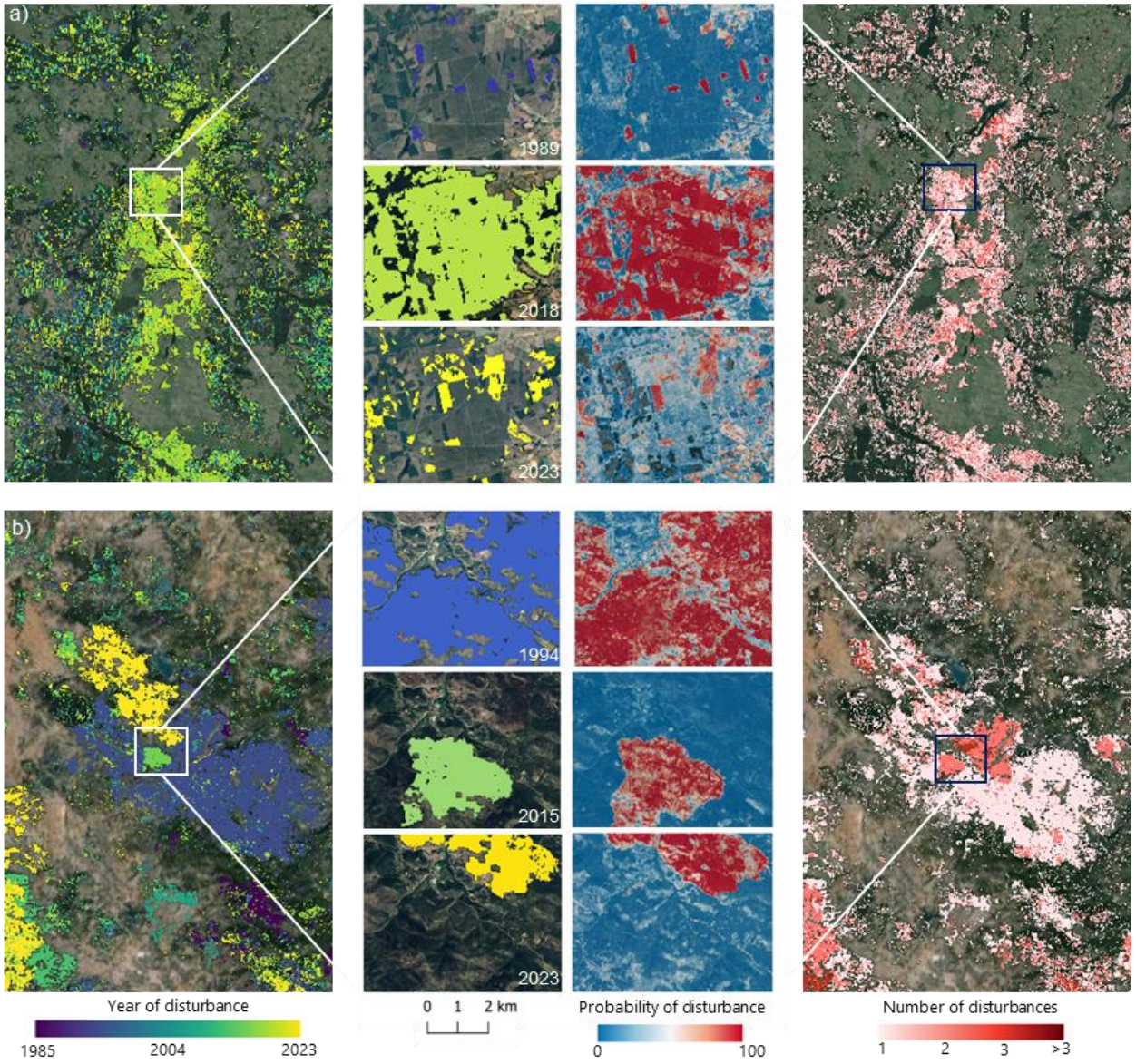

Figure B1. Examples of annual disturbances with its correspondent probability of disturbance and summary of number of disturbance events (underlying imagery ©Google). a) area affected by recent windstorm in north Poland that overlaps past and current harvest activities, b) multiple fire events in eastern Spain.

Table B1. Confusion matrix of disturbance detection assessment leaving out non-stand-replacing disturbances

	Reference data				
	Undisturbed	Disturbed	N	Commission errors (%)	Confidence intervals
Undisturbed	83233	74	83307	**0.1 %**	[99.83 - 99.97]
Disturbed	131	447	578	**22.66 %**	[74.30 - 82.87]
N	83364	521			
Omission errors (%)	**0.2**	**14.20**			
Confidence intervals	[99.72 - 99.85]	[79.98 - 88.27]			
F1 score	**0.99**	**0.81**	Overall accuracy = 90.7 % | Overall error = 9.28 %		

615 **Table B2. Confusion matrix of disturbance detection assessment per period**

	Reference data			
Period 1985-1989	Undisturbed	Disturbed	N	Commission errors (%)
Undisturbed	12220	21	12241	**0.17**
Disturbed	20	69	89	**22.47**
N	12240	90		
Omission errors (%)	**0.16**	**23.33**		
F1 score	**0.99**	**0.77**		

Period 1990-1999	Undisturbed	Disturbed	N	Commission errors (%)
Undisturbed	24627	52	24679	**0.21**
Disturbed	35	179	214	**16.35**
N	24662	231		
Omission errors (%)	**0.15**	**22.51**		
F1 score	**0.99**	**0.80**		

Period 2000-2018	Undisturbed	Disturbed	N	Commission errors (%)
Undisturbed	46404	134	46538	**0.28**
Disturbed	62	521	583	**10.63**
N	46466	651		
Omission errors (%)	**0.13**	**20.5**		
F1 score	**0.99**	**0.84**		

References

Abrams, M., Crippen, R., and Fujisada, H.: ASTER Global Digital Elevation Model (GDEM) and ASTER Global Water Body Dataset (ASTWBD), Remote Sens., 12, 1156, https://doi.org/10.3390/rs12071156, 2020.

d'Andrimont, R., Yordanov, M., Martinez-Sanchez, L., Eiselt, B., Palmieri, A., Dominici, P., Gallego, J., Reuter, H. I., Joebges, C., Lemoine, G., and Van Der Velde, M.: Harmonised LUCAS in-situ land cover and use database for field surveys from 2006 to 2018 in the European Union, Sci. Data, 7, 352, https://doi.org/10.1038/s41597-020-00675-z, 2020.

Baig, M. H. A., Zhang, L., Shuai, T., and Tong, Q.: Derivation of a tasselled cap transformation based on Landsat 8 at-satellite reflectance, Remote Sens. Lett., 5, 423–431, https://doi.org/10.1080/2150704X.2014.915434, 2014.

Banskota, A., Kayastha, N., Falkowski, M. J., Wulder, M. A., Froese, R. E., and White, J. C.: Forest Monitoring Using Landsat Time Series Data: A Review, Can. J. Remote Sens., 40, 362–384, https://doi.org/10.1080/07038992.2014.987376, 2014.

Belgiu, M. and Drăguţ, L.: Random forest in remote sensing: A review of applications and future directions, ISPRS J. Photogramm. Remote Sens., 114, 24–31, https://doi.org/10.1016/j.isprsjprs.2016.01.011, 2016.

Breidenbach, J., Ellison, D., Petersson, H., Korhonen, K. T., Henttonen, H. M., Wallerman, J., Fridman, J., Gobakken, T., Astrup, R., and Næsset, E.: Harvested area did not increase abruptly—how advancements in satellite-based mapping led to erroneous conclusions, Ann. For. Sci., 79, 2, https://doi.org/10.1186/s13595-022-01120-4, 2022.

Buma, B.: Disturbance interactions: characterization, prediction, and the potential for cascading effects, Ecosphere, 6, 1–15, https://doi.org/10.1890/ES15-00058.1, 2015.

Cardille, J. A., Perez, E., Crowley, M. A., Wulder, M. A., White, J. C., and Hermosilla, T.: Multi-sensor change detection for within-year capture and labelling of forest disturbance, Remote Sens. Environ., 268, 112741, https://doi.org/10.1016/j.rse.2021.112741, 2022.

Ceccherini, G., Duveiller, G., Grassi, G., Lemoine, G., Avitabile, V., Pilli, R., and Cescatti, A.: Abrupt increase in harvested forest area over Europe after 2015, Nature, 583, 72–77, https://doi.org/10.1038/s41586-020-2438-y, 2020.

Chawla, N. V., Bowyer, K. W., Hall, L. O., and Kegelmeyer, W. P.: SMOTE: Synthetic Minority Over-sampling Technique, J. Artif. Intell. Res., 16, 321–357, https://doi.org/10.1613/jair.953, 2002.

Chazdon, R. L., Brancalion, P. H. S., Laestadius, L., Bennett-Curry, A., Buckingham, K., Kumar, C., Moll-Rocek, J., Vieira, I. C. G., and Wilson, S. J.: When is a forest a forest? Forest concepts and definitions in the era of forest and landscape restoration, Ambio, 45, 538–550, https://doi.org/10.1007/s13280-016-0772-y, 2016.

Ciais, P., Schelhaas, M. J., Zaehle, S., Piao, S. L., Cescatti, A., Liski, J., Luyssaert, S., Le-Maire, G., Schulze, E.-D., Bouriaud, O., Freibauer, A., Valentini, R., and Nabuurs, G. J.: Carbon accumulation in European forests, Nat. Geosci., 1, 425–429, https://doi.org/10.1038/ngeo233, 2008.

Cohen, W., Healey, S., Yang, Z., Stehman, S., Brewer, C., Brooks, E., Gorelick, N., Huang, C., Hughes, M., Kennedy, R., Loveland, T., Moisen, G., Schroeder, T., Vogelmann, J., Woodcock, C., Yang, L., and Zhu, Z.: How Similar Are Forest Disturbance Maps Derived from Different Landsat Time Series Algorithms?, Forests, 8, 98, https://doi.org/10.3390/f8040098, 2017.

Cohen, W. B., Yang, Z., and Kennedy, R.: Detecting trends in forest disturbance and recovery using yearly Landsat time series: 2. TimeSync — Tools for calibration and validation, Remote Sens. Environ., 114, 2911–2924, https://doi.org/10.1016/j.rse.2010.07.010, 2010.

Cohen, W. B., Yang, Z., Healey, S. P., Kennedy, R. E., and Gorelick, N.: A LandTrendr multispectral ensemble for forest disturbance detection, Remote Sens. Environ., 205, 131–140, https://doi.org/10.1016/j.rse.2017.11.015, 2018.

Coops, N. C., Shang, C., Wulder, M. A., White, J. C., and Hermosilla, T.: Change in forest condition: Characterizing non-stand replacing disturbances using time series satellite imagery, For. Ecol. Manag., 474, 118370, https://doi.org/10.1016/j.foreco.2020.118370, 2020.

Crist, E. P.: A TM Tasseled Cap equivalent transformation for reflectance factor data, Remote Sens. Environ., 17, 301–306, https://doi.org/10.1016/0034-4257(85)90102-6, 1985.

Dutrieux, Loïc., Senf, C., Feret, J.-B., Malenovský, Zbyněk., and Beck, P. S. A.: JRC Expert Meeting on Remote Sensing: based bark beetle outbreak detection and mapping : held 22 November 2022 online, Publications Office of the European Union, Luxembourg, 2023.

European Commission, Joint Research Centre, Dutrieux, L., Beck, P., Herold, M., Olofsson, P., and Tsendbazar, N.: JRC expert meeting on accuracy assessment and comparison of forest disturbance products, Publications Office of the European Union, https://doi.org/10.2760/881978, 2023.

FAO: Global Forest Resources Assessment 2020: Main report, Rome, 2020.

Fassnacht, F. E., White, J. C., Wulder, M. A., and Næsset, E.: Remote sensing in forestry: current challenges, considerations and directions, For. Int. J. For. Res., 97, 11–37, https://doi.org/10.1093/forestry/cpad024, 2024.

Ferretti, M.: Europe needs a joined-up approach for monitoring and protecting its forests, Nature, 626, 954–954, 2024.

Ferretti, M., Gessler, A., Cools, N., Fleck, S., Guerrieri, R., Jakovljević, T., Nicolas, M., Nieminen, T. M., Pitar, D., Potočić, N., Raspe, S., Schaub, M., Schwärzel, K., Timmermann, V., Vejpustková, M., Vesterdal, L., Vanninen, P., Waldner, P., Zimmermann, L., and Sanders, T. G.: Perspectives: Resilient forests need joint forces for better inventorying and monitoring, For. Ecol. Manag., 561, 121875, https://doi.org/10.1016/j.foreco.2024.121875, 2024.

FOREST EUROPE: State of Europe's Forests, Ministerial Conference on the Protection of Forests in Europe, 2020.

Forman, G. and Scholz, M.: Apples-to-apples in cross-validation studies: pitfalls in classifier performance measurement, ACM SIGKDD Explor. Newsl., 12, 49–57, https://doi.org/10.1145/1882471.1882479, 2010.

Forzieri, G., Pecchi, M., Girardello, M., Mauri, A., Klaus, M., Nikolov, C., Rüetschi, M., Gardiner, B., Tomaštík, J., Small, D., Nistor, C., Jonikavicius, D., Spinoni, J., Feyen, L., Giannetti, F., Comino, R., Wolynski, A., Pirotti, F., Maistrelli, F., Savulescu, I., Wurpillot-Lucas, S., Karlsson, S., Zieba-Kulawik, K., Strejczek-Jazwinska, P., Mokroš, M., Franz, S., Krejci, L., Haidu, I., Nilsson, M., Wezyk, P., Catani, F., Chen, Y.-Y., Luyssaert, S., Chirici, G., Cescatti, A., and Beck, P. S. A.: A spatially explicit database of wind disturbances in European forests over the period 2000–2018, Earth Syst. Sci. Data, 12, 257–276, https://doi.org/10.5194/essd-12-257-2020, 2020.

Forzieri, G., Dutrieux, L. P., Elia, A., Eckhardt, B., Caudullo, G., Taboada, F. Á., Andriolo, A., Bălăcenoiu, F., Bastos, A., Buzatu, A., Dorado, F. C., Dobrovolný, L., Duduman, M., Fernandez-Carrillo, A., Hernández-Clemente, R., Hornero, A., Ionuț, S., Lombardero, M. J., Junttila, S., Lukeš, P., Marianelli, L., Mas, H., Mlčoušek, M., Mugnai, F., Nețoiu, C., Nikolov, C., Olenici, N., Olsson, P., Paoli, F., Paraschiv, M., Patočka, Z., Pérez-Laorga, E., Quero, J. L., Rüetschi, M., Stroheker, S.,

Nardi, D., Ferenčík, J., Battisti, A., Hartmann, H., Nistor, C., Cescatti, A., and Beck, P. S. A.: The Database of European Forest Insect and Disease Disturbances: DEFID2, Glob. Change Biol., 29, 6040–6065, https://doi.org/10.1111/gcb.16912, 2023.

Francini, S., McRoberts, R. E., Giannetti, F., Marchetti, M., Scarascia Mugnozza, G., and Chirici, G.: The Three Indices Three Dimensions (3I3D) algorithm: a new method for forest disturbance mapping and area estimation based on optical remotely sensed imagery, Int. J. Remote Sens., 42, 4693–4711, https://doi.org/10.1080/01431161.2021.1899334, 2021.

Francini, S., McRoberts, R. E., D'Amico, G., Coops, N. C., Hermosilla, T., White, J. C., Wulder, M. A., Marchetti, M., Mugnozza, G. S., and Chirici, G.: An open science and open data approach for the statistically robust estimation of forest disturbance areas, Int. J. Appl. Earth Obs. Geoinformation, 106, 102663, https://doi.org/10.1016/j.jag.2021.102663, 2022.

Francini, S., Hermosilla, T., Coops, N. C., Wulder, M. A., White, J. C., and Chirici, G.: An assessment approach for pixel-based image composites, ISPRS J. Photogramm. Remote Sens., 202, 1–12, https://doi.org/10.1016/j.isprsjprs.2023.06.002, 2023.

Franquesa, M., Vanderhoof, M. K., Stavrakoudis, D., Gitas, I. Z., Roteta, E., Padilla, M., and Chuvieco, E.: Development of a standard database of reference sites for validating global burned area products, Earth Syst. Sci. Data, 12, 3229–3246, https://doi.org/10.5194/essd-12-3229-2020, 2020.

Frantz, D.: FORCE—Landsat + Sentinel-2 Analysis Ready Data and Beyond, Remote Sens., 11, 1124, https://doi.org/10.3390/rs11091124, 2019.

Frantz, D., Roder, A., Udelhoven, T., and Schmidt, M.: Enhancing the Detectability of Clouds and Their Shadows in Multitemporal Dryland Landsat Imagery: Extending Fmask, IEEE Geosci. Remote Sens. Lett., 12, 1242–1246, https://doi.org/10.1109/LGRS.2015.2390673, 2015.

Frantz, D., Roder, A., Stellmes, M., and Hill, J.: An Operational Radiometric Landsat Preprocessing Framework for Large-Area Time Series Applications, IEEE Trans. Geosci. Remote Sens., 54, 3928–3943, https://doi.org/10.1109/TGRS.2016.2530856, 2016.

García, M. L. and Caselles, V.: Mapping burns and natural reforestation using Thematic Mapper data, Geocarto Int., 6, 31–37, 1991.

Gómez, C.: 4 Remote sensing for the Spanish forests in the 21st century: a review of 5 advances, needs, and opportunities. 6 Authors and affiliations, n.d.

Griffiths, P., Van Der Linden, S., Kuemmerle, T., and Hostert, P.: A Pixel-Based Landsat Compositing Algorithm for Large Area Land Cover Mapping, IEEE J. Sel. Top. Appl. Earth Obs. Remote Sens., 6, 2088–2101, https://doi.org/10.1109/JSTARS.2012.2228167, 2013.

Grünig, M., Seidl, R., and Senf, C.: Increasing aridity causes larger and more severe forest fires across Europe, Glob. Change Biol., 29, 1648–1659, https://doi.org/10.1111/gcb.16547, 2022.

Hammond, W. M., Williams, A. P., Abatzoglou, J. T., Adams, H. D., Klein, T., López, R., Sáenz-Romero, C., Hartmann, H., Breshears, D. D., and Allen, C. D.: Global field observations of tree die-off reveal hotter-drought fingerprint for Earth's forests, Nat. Commun., 13, 1761, https://doi.org/10.1038/s41467-022-29289-2, 2022.

Hansen, M. C., Potapov, P. V., Moore, R., Hancher, M., Turubanova, S. A., Tyukavina, A., Thau, D., Stehman, S. V., Goetz, S. J., Loveland, T. R., Kommareddy, A., Egorov, A., Chini, L., Justice, C. O., and Townshend, J. R. G.: High-Resolution Global Maps of 21st-Century Forest Cover Change, Science, 342, 850–853, https://doi.org/10.1126/science.1244693, 2013.

Hantson, S. and Chuvieco, E.: Evaluation of different topographic correction methods for Landsat imagery, Int. J. Appl. Earth Obs. Geoinformation, 13, 691–700, https://doi.org/10.1016/j.jag.2011.05.001, 2011.

Healey, S., Cohen, W., Zhiqiang, Y., and Krankina, O.: Comparison of Tasseled Cap-based Landsat data structures for use in forest disturbance detection, Remote Sens. Environ., 97, 301–310, https://doi.org/10.1016/j.rse.2005.05.009, 2005.

Hermosilla, T., Wulder, M. A., White, J. C., Coops, N. C., and Hobart, G. W.: Regional detection, characterization, and attribution of annual forest change from 1984 to 2012 using Landsat-derived time-series metrics, Remote Sens. Environ., 170, 121–132, https://doi.org/10.1016/j.rse.2015.09.004, 2015.

Hermosilla, T., Wulder, M. A., White, J. C., Coops, N. C., and Hobart, G. W.: Updating Landsat time series of surface-reflectance composites and forest change products with new observations, Int. J. Appl. Earth Obs. Geoinformation, 63, 104–111, https://doi.org/10.1016/j.jag.2017.07.013, 2017.

Hermosilla, T., Wulder, M. A., White, J. C., and Coops, N. C.: Prevalence of multiple forest disturbances and impact on vegetation regrowth from interannual Landsat time series (1985–2015), Remote Sens. Environ., 233, 111403, https://doi.org/10.1016/j.rse.2019.111403, 2019.

Hermosilla, T., Wulder, M. A., White, J. C., and Coops, N. C.: Land cover classification in an era of big and open data: Optimizing localized implementation and training data selection to improve mapping outcomes, Remote Sens. Environ., 268, 112780, https://doi.org/10.1016/j.rse.2021.112780, 2022.

Hirschmugl, M., Gallaun, H., Dees, M., Datta, P., Deutscher, J., Koutsias, N., and Schardt, M.: Methods for Mapping Forest Disturbance and Degradation from Optical Earth Observation Data: a Review, Curr. For. Rep., 3, 32–45, https://doi.org/10.1007/s40725-017-0047-2, 2017.

Hlásny, T., König, L., Krokene, P., Lindner, M., Montagné-Huck, C., Müller, J., Qin, H., Raffa, K. F., Schelhaas, M.-J., Svoboda, M., Viiri, H., and Seidl, R.: Bark Beetle Outbreaks in Europe: State of Knowledge and Ways Forward for Management, Curr. For. Rep., 7, 138–165, https://doi.org/10.1007/s40725-021-00142-x, 2021.

Huang, C., Goward, S. N., Masek, J. G., Thomas, N., Zhu, Z., and Vogelmann, J. E.: An automated approach for reconstructing recent forest disturbance history using dense Landsat time series stacks, Remote Sens. Environ., 114, 183–198, https://doi.org/10.1016/j.rse.2009.08.017, 2010.

Hughes, M., Kaylor, S., and Hayes, D.: Patch-Based Forest Change Detection from Landsat Time Series, Forests, 8, 166, https://doi.org/10.3390/f8050166, 2017.

Kennedy, R. E., Cohen, W. B., and Schroeder, T. A.: Trajectory-based change detection for automated characterization of forest disturbance dynamics, Remote Sens. Environ., 110, 370–386, https://doi.org/10.1016/j.rse.2007.03.010, 2007.

Kennedy, R. E., Yang, Z., and Cohen, W. B.: Detecting trends in forest disturbance and recovery using yearly Landsat time series: 1. LandTrendr — Temporal segmentation algorithms, Remote Sens. Environ., 114, 2897–2910, https://doi.org/10.1016/j.rse.2010.07.008, 2010.

Knutzen, F., Averbeck, P., Barrasso, C., Bouwer, L. M., Gardiner, B., Grünzweig, J. M., Hänel, S., Haustein, K., Johannessen, M. R., Kollet, S., Müller, M. M., Pietikäinen, J.-P., Pietras-Couffignal, K., Pinto, J. G., Rechid, D., Rousi, E., Russo, A., Suarez-Gutierrez, L., Veit, S., Wendler, J., Xoplaki, E., and Gliksman, D.: Impacts on and damage to European forests from the 2018–2022 heat and drought events, Nat. Hazards Earth Syst. Sci., 25, 77–117, https://doi.org/10.5194/nhess-25-77-2025, 2025.

Kobayashi, S. and Sanga-Ngoie, K.: The integrated radiometric correction of optical remote sensing imageries, Int. J. Remote Sens., 29, 5957–5985, https://doi.org/10.1080/01431160701881889, 2008.

Lecina-Diaz, J., Senf, C., Grünig, M., and Seidl, R.: Ecosystem services at risk from disturbance in Europe's forests, Glob. Change Biol., 30, e17242, https://doi.org/10.1111/gcb.17242, 2024.

Lindner, M., Maroschek, M., Netherer, S., Kremer, A., Barbati, A., Garcia-Gonzalo, J., Seidl, R., Delzon, S., Corona, P., Kolström, M., Lexer, M. J., and Marchetti, M.: Climate change impacts, adaptive capacity, and vulnerability of European forest ecosystems, For. Ecol. Manag., 259, 698–709, https://doi.org/10.1016/j.foreco.2009.09.023, 2010.

Liu, S., Brandt, M., Nord-Larsen, T., Chave, J., Reiner, F., Lang, N., Tong, X., Ciais, P., Igel, C., Pascual, A., Guerra-Hernandez, J., Li, S., Mugabowindekwe, M., Saatchi, S., Yue, Y., Chen, Z., and Fensholt, R.: The overlooked contribution of trees outside forests to tree cover and woody biomass across Europe, Sci. Adv., 2023.

Mandl, L., Viana-Soto, A., Seidl, R., Stritih, A., and Senf, C.: Unmixing-based forest recovery indicators for predicting long-term recovery success, Remote Sens. Environ., 308, 114194, https://doi.org/10.1016/j.rse.2024.114194, 2024.

Maroschek, M., Seidl, R., Poschlod, B., and Senf, C.: Quantifying patch size distributions of forest disturbances in protected areas across the European Alps, J. Biogeogr., 51, 368–381, https://doi.org/10.1111/jbi.14760, 2024.

McDowell, N. G., Allen, C. D., Anderson-Teixeira, K., Aukema, B. H., Bond-Lamberty, B., Chini, L., Clark, J. S., Dietze, M., Grossiord, C., Hanbury-Brown, A., Hurtt, G. C., Jackson, R. B., Johnson, D. J., Kueppers, L., Lichstein, J. W., Ogle, K., Poulter, B., Pugh, T. A. M., Seidl, R., Turner, M. G., Uriarte, M., Walker, A. P., and Xu, C.: Pervasive shifts in forest dynamics in a changing world, Science, 368, eaaz9463, https://doi.org/10.1126/science.aaz9463, 2020.

Miguel, S., Ruiz-Benito, P., Rebollo, P., Viana-Soto, A., Mihai, M. C., García-Martín, A., and Tanase, M.: Forest disturbance regimes and trends in continental Spain (1985- 2023) using dense Landsat time series, Environ. Res., 119802, https://doi.org/10.1016/j.envres.2024.119802, 2024.

Moisen, G. G., Meyer, M. C., Schroeder, T. A., Liao, X., Schleeweis, K. G., Freeman, E. A., and Toney, C.: Shape selection in Landsat time series: a tool for monitoring forest dynamics, Glob. Change Biol., 22, 3518–3528, https://doi.org/10.1111/gcb.13358, 2016.

Morresi, D., Maeng, H., Marzano, R., Lingua, E., Motta, R., and Garbarino, M.: High-Dimensional Detection of Landscape Dynamics: A Landsat Time Series-Based Algorithm for Forest Disturbance Mapping and Beyond, SSRN, https://doi.org/10.2139/ssrn.4703613, 2024.

Nabuurs, G.-J., Harris, N., Sheil, D., Palahi, M., Chirici, G., Boissière, M., Fay, C., Reiche, J., and Valbuena, R.: Glasgow forest declaration needs new modes of data ownership, Nat. Clim. Change, 12, 415–417, https://doi.org/10.1038/s41558-022-01343-3, 2022.

Oeser, J., Pflugmacher, D., Senf, C., Heurich, M., and Hostert, P.: Using Intra-Annual Landsat Time Series for Attributing Forest Disturbance Agents in Central Europe, Forests, 8, 251, https://doi.org/10.3390/f8070251, 2017.

Olofsson, P., Foody, G. M., Herold, M., Stehman, S. V., Woodcock, C. E., and Wulder, M. A.: Good practices for estimating area and assessing accuracy of land change, Remote Sens. Environ., 148, 42–57, https://doi.org/10.1016/j.rse.2014.02.015, 2014.

Orsi, F., Ciolli, M., Primmer, E., Varumo, L., and Geneletti, D.: Mapping hotspots and bundles of forest ecosystem services across the European Union, Land Use Policy, 99, 104840, https://doi.org/10.1016/j.landusepol.2020.104840, 2020.

Palahí, M., Valbuena, R., Senf, C., Acil, N., Pugh, T. A. M., Sadler, J., Seidl, R., Potapov, P., Gardiner, B., Hetemäki, L., Chirici, G., Francini, S., Hlásny, T., Lerink, B. J. W., Olsson, H., González Olabarria, J. R., Ascoli, D., Asikainen, A., Bauhus, J., Berndes, G., Donis, J., Fridman, J., Hanewinkel, M., Jactel, H., Lindner, M., Marchetti, M., Marušák, R., Sheil, D., Tomé, M., Trasobares, A., Verkerk, P. J., Korhonen, M., and Nabuurs, G.-J.: Concerns about reported harvests in European forests, Nature, 592, E15–E17, https://doi.org/10.1038/s41586-021-03292-x, 2021.

Patacca, M., Lindner, M., Lucas-Borja, M. E., Cordonnier, T., Fidej, G., Gardiner, B., Hauf, Y., Jasinevičius, G., Labonne, S., Linkevičius, E., Mahnken, M., Milanovic, S., Nabuurs, G., Nagel, T. A., Nikinmaa, L., Panyatov, M., Bercak, R., Seidl, R., Ostrogović Sever, M. Z., Socha, J., Thom, D., Vuletic, D., Zudin, S., and Schelhaas, M.: Significant increase in natural disturbance impacts on European forests since 1950, Glob. Change Biol., 29, 1359–1376, https://doi.org/10.1111/gcb.16531, 2023.

Pedregosa, F., Varoquaux, G., Gramfort, A., Michel, V., Thirion, B., Grisel, O., Blondel, M., Prettenhofer, P., Weiss, R., and Dubourg, V.: Scikit-learn: Machine learning in Python, J. Mach. Learn. Res., 12, 2825–2830, 2011.

Pflugmacher, D., Rabe, A., Peters, M., and Hostert, P.: Mapping pan-European land cover using Landsat spectral-temporal metrics and the European LUCAS survey, Remote Sens. Environ., 221, 583–595, https://doi.org/10.1016/j.rse.2018.12.001, 2019.

Pugh, T. A. M., Arneth, A., Kautz, M., Poulter, B., and Smith, B.: Important role of forest disturbances in the global biomass turnover and carbon sinks, Nat. Geosci., 12, 730–735, https://doi.org/10.1038/s41561-019-0427-2, 2019.

Reinosch, E., Backa, J., Adler, P., Deutscher, J., Eisnecker, P., Hoffmann, K., Langner, N., Puhm, M., Rüetschi, M., Straub, C., Waser, L. T., Wiesehahn, J., and Oehmichen, K.: Detailed validation of large-scale Sentinel-2-based forest disturbance maps across Germany, For. Int. J. For. Res., cpae038, https://doi.org/10.1093/forestry/cpae038, 2024.

Roy, D. P., Kovalskyy, V., Zhang, H. K., Vermote, E. F., Yan, L., Kumar, S. S., and Egorov, A.: Characterization of Landsat-7 to Landsat-8 reflective wavelength and normalized difference vegetation index continuity, Remote Sens. Environ., 185, 57–70, https://doi.org/10.1016/j.rse.2015.12.024, 2016.

Saarikoski, H., Jax, K., Harrison, P. A., Primmer, E., Barton, D. N., Mononen, L., Vihervaara, P., and Furman, E.: Exploring operational ecosystem service definitions: The case of boreal forests, Ecosyst. Serv., 14, 144–157, https://doi.org/10.1016/j.ecoser.2015.03.006, 2015.

Sabatini, F. M., Burrascano, S., Keeton, W. S., Levers, C., Lindner, M., Pötzschner, F., Verkerk, P. J., Bauhus, J., Buchwald, E., Chaskovsky, O., Debaive, N., Horváth, F., Garbarino, M., Grigoriadis, N., Lombardi, F., Marques Duarte, I., Meyer, P., Midteng, R., Mikac, S., Mikoláš, M., Motta, R., Mozgeris, G., Nunes, L., Panayotov, M., Ódor, P., Ruete, A., Simovski, B., Stillhard, J., Svoboda, M., Szwagrzyk, J., Tikkanen, O., Volosyanchuk, R., Vrska, T., Zlatanov, T., and Kuemmerle, T.: Where are Europe's last primary forests?, Divers. Distrib., 24, 1426–1439, https://doi.org/10.1111/ddi.12778, 2018.

Sebald, J., Senf, C., and Seidl, R.: Human or natural? Landscape context improves the attribution of forest disturbances mapped from Landsat in Central Europe, Remote Sens. Environ., 262, 112502, https://doi.org/10.1016/j.rse.2021.112502, 2021.

Seidl, R.: The Shape of Ecosystem Management to Come: Anticipating Risks and Fostering Resilience, BioScience, 64, 1159–1169, https://doi.org/10.1093/biosci/biu172, 2014.

Seidl, R. and Rammer, W.: Climate change amplifies the interactions between wind and bark beetle disturbances in forest landscapes, Landsc. Ecol., 32, 1485–1498, https://doi.org/10.1007/s10980-016-0396-4, 2017.

Seidl, R. and Senf, C.: Changes in planned and unplanned canopy openings are linked in Europe's forests, Nat. Commun., 15, 4741, https://doi.org/10.1038/s41467-024-49116-0, 2024.

Senf, C.: Manually interpreted reference data on forest disturbances across Europe [Dataset], Zenodo, https://doi.org/10.5281/zenodo.3561925, 2019.

Senf, C.: Seeing the System from Above: The Use and Potential of Remote Sensing for Studying Ecosystem Dynamics, Ecosystems, 25, 1719–1737, https://doi.org/10.1007/s10021-022-00777-2, 2022.

Senf, C. and Seidl, R.: Natural disturbances are spatially diverse but temporally synchronized across temperate forest landscapes in Europe, Glob. Change Biol., 24, 1201–1211, https://doi.org/10.1111/gcb.13897, 2018.

Senf, C. and Seidl, R.: Mapping the forest disturbance regimes of Europe, Nat. Sustain., 4, 63–70, https://doi.org/10.1038/s41893-020-00609-y, 2021a.

Senf, C. and Seidl, R.: Storm and fire disturbances in Europe: Distribution and trends, Glob. Change Biol., 27, 3605–3619, https://doi.org/10.1111/gcb.15679, 2021b.

Senf, C., Pflugmacher, D., Zhiqiang, Y., Sebald, J., Knorn, J., Neumann, M., Hostert, P., and Seidl, R.: Canopy mortality has doubled in Europe's temperate forests over the last three decades, Nat. Commun., 9, 4978, https://doi.org/10.1038/s41467-018-07539-6, 2018.

Senf, C., Sebald, J., and Seidl, R.: Increasing canopy mortality affects the future demographic structure of Europe's forests, One Earth, 4, 749–755, https://doi.org/10.1016/j.oneear.2021.04.008, 2021.

Sommerfeld, A., Senf, C., Buma, B., D'Amato, A. W., Després, T., Díaz-Hormazábal, I., Fraver, S., Frelich, L. E., Gutiérrez, Á. G., Hart, S. J., Harvey, B. J., He, H. S., Hlásny, T., Holz, A., Kitzberger, T., Kulakowski, D., Lindenmayer, D., Mori, A. S., Müller, J., Paritsis, J., Perry, G. L. W., Stephens, S. L., Svoboda, M., Turner, M. G., Veblen, T. T., and Seidl, R.: Patterns and drivers of recent disturbances across the temperate forest biome, Nat. Commun., 9, 4355, https://doi.org/10.1038/s41467-018-06788-9, 2018.

Stahl, A. T., Andrus, R., Hicke, J. A., Hudak, A. T., Bright, B. C., and Meddens, A. J. H.: Automated attribution of forest disturbance types from remote sensing data: A synthesis, Remote Sens. Environ., 285, 113416, https://doi.org/10.1016/j.rse.2022.113416, 2023.

Stritih, A., Senf, C., Seidl, R., Grêt-Regamey, A., and Bebi, P.: The impact of land-use legacies and recent management on natural disturbance susceptibility in mountain forests, For. Ecol. Manag., 484, 118950, https://doi.org/10.1016/j.foreco.2021.118950, 2021.

Thom, D. and Seidl, R.: Natural disturbance impacts on ecosystem services and biodiversity in temperate and boreal forests, Biol. Rev., 91, 760–781, https://doi.org/10.1111/brv.12193, 2016.

Tucker, C. J.: Red and photographic infrared linear combinations for monitoring vegetation, Remote Sens. Environ., 8, 127–150, 1979.

Turner, M. G. and Seidl, R.: Novel Disturbance Regimes and Ecological Responses, Annu. Rev. Ecol. Evol. Syst., 54, 63–83, https://doi.org/10.1146/annurev-ecolsys-110421-101120, 2023.

Turubanova, S., Potapov, P., Hansen, M. C., Li, X., Tyukavina, A., Pickens, A. H., Hernandez-Serna, A., Arranz, A. P., Guerra-Hernandez, J., Senf, C., Häme, T., Valbuena, R., Eklundh, L., Brovkina, O., Navrátilová, B., Novotný, J., Harris, N., and

Stolle, F.: Tree canopy extent and height change in Europe, 2001–2021, quantified using Landsat data archive, Remote Sens. Environ., 298, 113797, https://doi.org/10.1016/j.rse.2023.113797, 2023.

Valavi, R., Elith, J., Lahoz-Monfort, J. J., and Guillera-Arroita, G.: blockCV: An r package for generating spatially or environmentally separated folds for k-fold cross-validation of species distribution models, Methods Ecol. Evol., 10, 225–232, https://doi.org/10.1111/2041-210X.13107, 2019.

Valavi, R., Guillera-Arroita, G., Lahoz-Monfort, J. J., and Elith, J.: Predictive performance of presence-only species distribution models: a benchmark study with reproducible code, Ecol. Monogr., 92, e01486, https://doi.org/10.1002/ecm.1486, 2022.

Verbesselt, J., Hyndman, R., Newnham, G., and Culvenor, D.: Detecting trend and seasonal changes in satellite image time series, Remote Sens. Environ., 114, 106–115, https://doi.org/10.1016/j.rse.2009.08.014, 2010.

Viana-Soto, A. and Senf, C.: European Forest Disturbance Atlas (2.1.1.), https://doi.org/10.5281/zenodo.13333034, 2024.

Wulder, M. A., Roy, D. P., Radeloff, V. C., Loveland, T. R., Anderson, M. C., Johnson, D. M., Healey, S., Zhu, Z., Scambos, T. A., Pahlevan, N., Hansen, M., Gorelick, N., Crawford, C. J., Masek, J. G., Hermosilla, T., White, J. C., Belward, A. S., Schaaf, C., Woodcock, C. E., Huntington, J. L., Lymburner, L., Hostert, P., Gao, F., Lyapustin, A., Pekel, J.-F., Strobl, P., and Cook, B. D.: Fifty years of Landsat science and impacts, Remote Sens. Environ., 280, 113195, https://doi.org/10.1016/j.rse.2022.113195, 2022.

Wulder, M. A., Hermosilla, T., White, J. C., Bater, C. W., Hobart, G., and Bronson, S. C.: Development and implementation of a stand-level satellite-based forest inventory for Canada, For. Int. J. For. Res., cpad065, https://doi.org/10.1093/forestry/cpad065, 2024.

Zhao, K., Wulder, M. A., Hu, T., Bright, R., Wu, Q., Qin, H., Li, Y., Toman, E., Mallick, B., Zhang, X., and Brown, M.: Detecting change-point, trend, and seasonality in satellite time series data to track abrupt changes and nonlinear dynamics: A Bayesian ensemble algorithm, Remote Sens. Environ., 232, 111181, https://doi.org/10.1016/j.rse.2019.04.034, 2019.

Zhu, Z.: Change detection using landsat time series: A review of frequencies, preprocessing, algorithms, and applications, ISPRS J. Photogramm. Remote Sens., 130, 370–384, https://doi.org/10.1016/j.isprsjprs.2017.06.013, 2017.

Zhu, Z. and Woodcock, C. E.: Object-based cloud and cloud shadow detection in Landsat imagery, Remote Sens. Environ., 118, 83–94, https://doi.org/10.1016/j.rse.2011.10.028, 2012.

Zhu, Z. and Woodcock, C. E.: Automated cloud, cloud shadow, and snow detection in multitemporal Landsat data: An algorithm designed specifically for monitoring land cover change, Remote Sens. Environ., 152, 217–234, https://doi.org/10.1016/j.rse.2014.06.012, 2014a.

Zhu, Z. and Woodcock, C. E.: Continuous change detection and classification of land cover using all available Landsat data, Remote Sens. Environ., 144, 152–171, https://doi.org/10.1016/j.rse.2014.01.011, 2014b.